universität wien

MASTERARBEIT / MASTER'S THESIS

Titel der Masterarbeit / Title of the Master's Thesis

„Evaluation of alternative fluorophores for fluorescence *in situ* hybridization in microbial ecology"

verfasst von / submitted by

Adrian Christoph Berger, BSc

angestrebter akademischer Grad / in partial fulfilment of the requirements for the degree of

Master of Science (MSc)

Wien, 2016 / Vienna, 2016

Studienkennzahl lt. Studienblatt / degree programme code as it appears on the student record sheet:	A 066 830
Studienrichtung lt. Studienblatt / degree programme as it appears on the student record sheet:	Molekulare Mikrobiologie, mikrobielle Ökologie und Immunbiologie
Betreut von / Supervisor:	Assoz. Prof. Dipl.-Biol. Dr. Holger Daims

TABLE OF CONTENTS

ABSTRACT

Fluorescence *in situ* hybridization (FISH) with rRNA-targeted olignoucleotides is a very powerful and versatile tool for the verification, visualization and enumeration of microorganisms in environmental and medical samples. As this cultivation-independent technique also offers the possibility of visualizing the *in situ* spatial arrangement of microbes in the environment and to each other, hereby revealing potential antagonistic or mutualistic lifestyles, it represents an essential method that helps to understand complex microbial interactions. However, due to intrinsic limitations of microscopy (fixed excitation wavelengths, fixed filters and detectors) in the past, researchers were constraint to the simultaneous visualization of a few different microbial taxa. Although several attempts to circumvent this limitation have been made by applying probes equipped with binary dye combinations or multiple, mono- labelled probes competing for the same target site, they all suffer from a reduced sensitivity and thus might be prone to wrong cell assignment. We here present a novel, robust, and straight-forward multicolour FISH approach that fully exploits the steplessly tunable white light laser (WLL) technology and the introduction of alternative fluorophores. As a biological proof of principle, this method was used to visualize the (micro)- diversity of the nitrifying community within activated sludge of the full- scale wastewater treatment plant (WWTP) Ingolstadt, Germany. By this, eight different microbial taxa could successfully be visualized, whereat six target groups could be detected simultaneously within one field of view. Fluorescence intensity measurements further revealed that two alternative dyes clearly exceeded the brightness of the carbocyanine dye Cy3 by a factor of 1.45 and 1.55, respectively. Thus this study not only offers a rash of new and attractive alternative dyes that are compatible with FISH, but also depicts an easy and robust multicolour FISH approach with increased sensitivity that will particularly be helpful in the future for the assessment of complex microbial communities.

Keywords: Fluorescence *in situ* hybridization, multicolour FISH, alternative fluorophores, white light laser, activated sludge, microdiversity, *Nitrospira*

1. INTRODUCTION

A SHORT RETROSPECTIVE

Today it is generally accepted, that there is a huge discrepancy between the number of microbial taxa that grow under laboratory conditions, and those thriving in natural environments. Additionally, those organisms growing under artificial, usually high- nutrient growth media at moderate temperatures, as a rule, are neither numerically, nor functionally dominant in the natural environment. These easily cultivable microorganisms are often referred to as "microbial weeds" and are estimated to account for less than 1% of all microbial species. This phenomenon is commonly known as the "great plate- count anomaly" **(Staley & Konopka, 1985)** and has caused many incomprehension among microbiologists in the past.

Before the pioneering work of Carl Woese and colleagues **(Fox et al., 1977; Woese & Fox, 1977; Woese, 1987)** microbial classification and taxonomy was solely based on morphology, gram staining, substrate requirements, pathogenic potential and so forth. Their newly introduced approach of comparative sequence analysis of genes encoding the ribosomal ribonucleic acid (rRNA) molecules was an outstanding attempt to reconstruct microbial evolution and has nowadays become an integral part of species description of bacteria and archaea. Retrieved 16S rRNA gene sequences are fed into a so-called phylogenetic tree which depicts the evolutionary distance to other known species, and hence identifies its evolutionary relationship to other organism, ranging from subspecies **(Amann et al., 1990)** to kingdom level **(Giovannoni et al., 1988**).

In the mid- 1980s, two publications outlined an extended molecular approach, which for the first time erased the need for cultivation in order to determine the sequence of the 16S rRNA gene **(Pace et al., 1985; Olsen et al., 1986)**. Since the introduction of the rRNA-approach, it is basically possible to extract bulk deoxyribonucleic acid (DNA) directly from the environment and subsequently amplify 16S rRNA gene sequences of a respective environmental sample using PCR with highly degenerated primers and cloning. Unfortunately, due to the many intrinsic biases regarding DNA-extraction and polymerase chain reaction (PCR), no quantitative predictions or conclusions about individual *in situ* species abundances can be made by applying this technique.

To overcome this issue, one can apply 16S rRNA-targeted nucleic acid probes specific for the organisms of interest in order to visualize and quantify the target group in the natural environment. This technique, referred to as fluorescence *in situ* hybridization (FISH), brings the rRNA approach to a full

circle and makes it a powerful tool for identification, enumeration and visualization of microbes in the environment **(Amann et al., 1995)**.

The rationale behind the usage of the rRNA molecule as target molecule for whole cell hybridization is the following: (i) they are ubiquitously distributed among all living organisms in very high copy numbers, approximately ranging from 10^3- 10^5 ribosomes per cell, (ii) they are naturally amplified within microbes as integral part of the ribosomes, and (iii) they possess super variable and highly conserved regions which makes them ideal for probe design **(Amann et al., 1990; Amann et al., 1995; Daims et al., 2005).**

1.1. FLUORESCENCE *IN SITU* HYBRIDIZATION

1.1.1. THE BASICS

A typical FISH protocol is comprised of at least 4 steps: the fixation and permeabilization of the cells, hybridization of the probe with its target on the rRNA, a washing step in order to remove unbound and excessive probes and, finally, the detection of labelled cells by microscopy or flow cytometry **(Amann et al., 1995; Daims et al., 2005; Wallner et al., 1993; DeLong et al., 1989)**.

The oligonucleotide probes applied in FISH protocols usually are between 15 and 30 nucleotides in length, complementary to the 16S rRNA target sequence and covalently conjugated to a single fluorescent dye molecule at the 5'- end of the probe. Commonly used fluorophores are e.g. fluorescein, tetramethylrhodamine, Texas red and increasingly, due to very high quantum yields, carbocyanine dyes like Cy3 and Cy5 **(Glöckner et al., 1996; Randolph & Wagner, 1997; Southwick et al., 1990)**.

DeLong and colleagues, in the late 1980's, were the first to successfully design and apply fluorescently labelled oligonucleotide probes to distinct the 3 domains of life, bacteria, archaea and eukarya **(DeLong et al., 1989).** Since then, FISH has become an relatively easy to apply and powerful tool for the investigation of natural and man- made systems **(Burggraf et al., 1994; Glöckner et al., 1996; Kempf et al., 2000; Spring et al., 1992; Wagner et al., 2003)**. However, although the standard FISH protocols are quite robust and straight-forward, there were many obstacles in the past that hindered successful hybridization and detection.

1.1.2. DRAWBACKS & RESTRICTIONS AND HOW TO CIRCUMVENT THEM

1.1.2.1. RIBOSOMAL YIELD AND CELL WALL PERMEABILITY

First of all, the detection limit of FISH with a requirement for at least 10^3- 10^4 cells per ml of sample is relatively high. In case of aquatic samples, one can easily concentrate cell densities by a simple pre-filtration step or by stimulating growth with a short pre-incubation, although the latter possibility should not be used for quantitative conclusions, since it will probably bias the community composition **(Amann et al., 1995; Daims et al., 2005)**.

Unfortunately, many microbes tend to possess a cell envelope that is, after fixation with the standard fixative formaldehyde, impermeable to the labelled probes. As a consequence, these organisms fail to show a FISH signal. This is especially true for Gram-positive bacteria and many archaea. In this cases, permeability can be improved using either ethanol as fixative, or by the application of enzymes such

as lysozyme, proteases, or the use of detergents and even short- term incubations with hydrochloric acid **(Burggraf et al., 1994; Zarda et al., 1991)**.

Further, it has been postulated that by applying standard mono-labelled probes, a few thousand ribosomes per cell are required to obtain a FISH signal **(Amann et al., 1995).** These conditions, however, are quite frequently not met in practice due to small cell size or low metabolic activity **(Colwell et al., 1985)**. In such cases FISH detection might become possible using either catalyzed reported deposition (CARD-FISH) **(Schönhuber et al., 1997)**, or double labeling of oligonucleotide probes (DOPE-FISH) **(Stoecker et al., 2010)**. Alternatively one could also apply peptide nucleic acid (PNA) probes **(Perry-O'Keefe et al., 2001; Worden et al., 2000),** polyribonucleotide probes **(Pernthaler et al., 2002)** or locked nucleic acid (LNA)-incorporated oligodeoxynucleotide probes (LNA/DNA probes) **(Kubota et al., 2006)**. It has been shown that the sensitivity of CARD-FISH and the appliance of polyribonucleotides were 26- to 41-fold and 10- to 50-fold higher than that of conventional FISH, respectively **(Schönhuber et al., 1997; Delong et al., 1999)**.

1.1.2.2. ACCESSIBILITY OF THE rRNA MOLECULE AND PROBE DESIGN

In the past, especially in the beginning of FISH, probe design, which ultimately strongly determines probe accessibility to its target, was prone to many trial and error attempts and restricted to empirical findings. Fuchs and co-workers were the first ones to conduct a systematic and comprehensive analysis of the *in situ* accessibility of *E. coli*'s 16S rRNA for fluorescently labelled oligonucleotide probes **(Fuchs et al., 1998)**. All retrieved fluorescence intensities (the fluorophore was fluorescein) obtained with more than 200 probes were grouped according to their relative fluorescence into six classes of brightness. Three years later, the same procedure was performed using Cy3 as the fluorescent dye and the 23S rRNA as target molecule, respectively **(Fuchs et al., 2001).** These two studies unequivocally demonstrated, that the accessibility of the respective probe target sites, and thus signal intensities strongly differed due to the higher- order structure of the ribosome **(Fuchs et al., 2001),** which includes rRNA-rRNA interactions, as well as interactions of the rRNA with ribosomal proteins **(Ban et al., 1999; Clemons et al., 1999)**.

In 2003, another study investigated the *in situ* accessibility of the small subunit rRNA including all members of the three domains **(Behrens et al., 2003)**. By using *E. coli* as the bacterial representative, quite significant differences in signal intensities were obtained between the fluorescein **(Fuchs et al., 1998)** and the Cy3 **(Behrens et al., 2003)** map. While this phenomenon usually is related to specific interactions of the fluorophore with the nucleotides **(Behrens et al., 2004; Crockett & Wittwer, 2001; Nazarenko et al., 2002; Torimura et al., 2001; Zahavy & Fox, 1999; Yarmoluk et al., 2001)**, it is also possible that proteins might act as quencher and thus reduce fluorescence **(Yilmaz & Noguera, 2004)**.

Additionally, Fuchs and colleagues point out, that due to the more linear structure of the Cy3 dye steric hindrances might be reduced, and as a consequence probe binding to its target is facilitated **(Fuchs et al., 2000).** Another study from 2001 also demonstrated the successful unlocking of previously inaccessible target sites using Cy3 or Cy5 as fluorescent dyes, instead of fluorescein **(Stoecker et al., 2010)**. Again, the authors contribute this improved probe accessibility to the chemical structure of the fluorophore, which apparently helps to resolve secondary or tertiary structures.

Inspired by preliminary findings of **Niemeyer et al. (1998)**, Fuchs and colleagues in 2000 introduced the appliance of unlabelled, so-called "helper" oligonucleotides that bind adjacent to the probe target site where they are thought to prevent the reestablishment of the native secondary structure, and thereby make the target sites accessible for probe binding. Indeed it could be shown that the use of one single helper increased signal brightness by up to 25-fold and that the helper effect rapidly decreases with increasing distance to the probe target site **(Fuchs et al., 2000)**.

Regarding probe design, especially the studies of Yilmaz et al**. (Yilmaz & Noguera, 2004, 2007; Yilmaz et al., 2008, 2011)** turned out to be helpful. They developed a model of FISH that is based on the thermodynamic affinity of a probe to its target during nucleic acid hybridization. The thermodynamic affinity is defined as the overall free energy change (ΔG° overall) for a given reaction mechanism including all occurring inter- (DNA-rRNA) and intraspecific (rRNA-rRNA) interactions, respectively, and turned out to be a powerful predictor of signal intensity **(Yilmaz & Noguera, 2004)**. These findings, together with results obtained from their follow-up studies about the calculation of dissociation profiles for probes **(Yilmaz & Noguera, 2007)** and the mismatch stability **(Yilmaz et al., 2008)** were then brought together in a web tool called mathFISH, a powerful algorithm that aids *in silico* design and evaluation of probes **(Yilmaz et al., 2011)**. In another study, they could further demonstrate that extension of the hybridization period up to 96 hours dramatically increases signal brightness, and thus there are no truly inaccessible target regions in the rRNA. In practice however, one has to find a trade-off between incubation time and signal intensity, since nonspecific binding may increase background fluorescence **(Yilmaz et al., 2006)**.

And finally, in order to circumvent a fundamental problem in microbial ecology, namely the lack of pure cultures, Schramm et al. introduced an elegant way to evaluate target site accessibility and optimal hybridization conditions in case there is no pure culture available **(Schramm et al., 2002)**. This technique, referred to as Clone-FISH, exploits the use of plasmids containing a T7 polymerase promoter and *E. coli* host cells with an isopropyl- b- D- thiogalactopyranoside (IPTG)- inducible T7 RNA polymerase in order to transcribe rRNA genes cloned from the environment.

1.1.3. POTENTIAL AND POWER OF FISH

1.1.3.1. ELUCIDATION OF METABOLICALLY ACTIVE ORGANISMS

First described by **Schäechter et al. (1958)**, and later also confirmed by several other research groups **(Binder & Liu, 1998; DeLong et al., 1989)** it turned out, that ribosomes which represent the protein factories within all cells, in several organisms like the *Synechococcus* strain WH8101 or *E. coli,* show a direct correlation between their cellular number and the general metabolic activity or growth rate. With this direct correlation it would basically be possible, not only to identify and visualize a certain organism of interest within its native environment, but also to make conclusions about its respective metabolic activity. However, investigations of **Wagner et al. (1995)** revealed a different story for representatives of the ammonia-oxidizing community from activated sludge and trickling filter biofilms. According to their results, ammonia-oxidizing microorganisms were able to maintain their ribosomal content upon inhibition for a period of up to five hours. **Flärdh and co- workers (1992)** came to similar results investigating the marine *Vibrio* sp. Strain CCUG 15956. They could show, that ribosomes were lost relatively slow (a half-life time of 79 h) and that they exist in large excess over the apparent demand for protein synthesis upon prolonged starvation. Since the ribosomal yield apparently can't be used for conclusions about activity, microbial ecologists came up with several suggestions:

One solution to this problem, albeit quite tricky due to the intrinsic instability of the rRNA precursor molecule, might be a FISH protocol with probes specifically targeting the intergenic spacer region in addition to or instead of the rRNA **(Pernthaler & Amann, 2004; Schmid et al., 2001)**. Since new ribosomes are solely being synthesized during metabolic activity, the intergenic spacer region reflects activity more accurately than the 16S or 23S rRNA. However, due to the instability of its target and its proposed leakage from the cells during hybridization, is still far from routine **(Hoshino et al., 2008).**

In 1999, Lee and colleagues for the first time successfully combined FISH and microautoradiography (FISH-MAR), enabling the analysis of metabolic activity of microbes *in situ* by direct visualization of substrate uptake **(Lee et al., 1999)**. One really critical aspect of this method clearly is the use of radioactive substrates and that the sensitivity of this technique is too low, as to resolve activity on a single cell level. Recently, however, two very promising protocols (Raman-FISH, NanoSIMS-FISH) have been published, that extend and complement technologies such as FISH-MAR and stable isotope probing (SIP) so that they can be applied at the resolution of single cells and additionally are quantitative **(Huang et al., 2007; Li et al., 2008)**. Furthermore, none of the latter mentioned techniques use radiolabelled substrates and, in addition Raman-FISH is non-destructive.

1.1.3.2. SPATIAL IN SITU VISUALIZATION OF MICROBES

Probably the most powerful and characteristic feature of FISH is depicted in its ability to make conclusions about the spatial distribution and potential interactions between different microbes or microbial guilds. Since co-localization of microbial populations are signposts for interactions, the spatial organization of complex communities is crucial for the overall understanding of microbial community dynamics, nutrient fluxes and tight inter- and intraspecific relationships **(Welch et al., 2016)**. Some studies could for example show, that several microbial guilds like the ammonia oxidizing bacteria (AOB) and the nitrite oxidizing bacteria (NOB) who, due to their mutualistic, syntrophic relationship, theoretically should appear in close vicinity to each other, really cluster together **(Daims et al., 2006; Juretschko et al., 1998)**. Furthermore, Daims and colleagues could show that *Nitrospira* microcolonies are interspersed with a network of cell-free channels that is supposed to aid the diffusion of nitrite, gases and metabolic waste compounds through the aggregates **(Daims et al., 2001)**. Spatial *in situ* visualization is of great importance not only for interspecies interactions, but also for the analysis of intraspecies relationships, e.g. when dealing with different strains of a certain species. Since the introduction of the term "microdiversity", which defines genetically closely related, but metabolically potentially distinct microbes, a hitherto unanticipated vast diversity in regard to metabolic versatility and function was discovered on a species level **(Moore et al., 1998)**. After this initial discovery, several other studies further investigated this issue and it turned out that the phenomenon of microdiversity seems to be quite common in marine systems **(Fuhrman & Campbell, 1998; Garcia- Martinez & Rodriguez- Valera, 2000; Kashtan et al., 2014; Moore et al., 1998; Woebken et al., 2008)**, freshwater **(Jaspers & Overmann, 2004)**, dental plaques **(Welch et al., 2016)** and within the nitrifying community, especially within the metabolically quite diverse genus *Nitrospira* **(Daims et al., 2001; 2006; Maixner et al., 2006).** A study on microdiversity within *Nitrospira* by **Gruber-Dorninger et al. (2015)** revealed, that several phylogenetically closely related clusters (16S rRNA identities between 95.8-99.6%) stably coexisted in one environment for periods of several years. Interestingly, the sub-clusters showed different preferences regarding nitrite concentrations, the utilization of formate as substrate and the spatial co-aggregation with AOB as mutualistic partners, which was monitored with newly designed probes.

The significance of these findings about microdiversity is, that the environment surrounding a given microbe, has previously unanticipated, massive impacts on each individual cell. Key components affecting the microscale environment are microbes themselves, as they serve as substrate for attachment of other microbes, create spatial structure and fine-scale gradients of diffusible metabolites **(Welch et al., 2016)**. Close proximity or physical contact between two microbes can substantially alter their physiology, for example conferring on a NOB the ability to survive in habitats

where nitrite is absent in higher concentrations, but AOB, through the oxidation of ammonia to nitrite, provide the substrate for NOB in close vicinity. Thus, a holistic understanding of the physiology of microbial key players of any kind, depends on knowing the identity of the surrounding partners with which they interact. Thus, this clearly raises the need for the visualization of as many taxa per experiment as possible.

1.1.4. MULTICOLOUR FISH

1.1.4.1. PREVIOUS MULTICOLOUR-FISH APPROACHES

In theory, rRNA-targeted probes could be designed and simultaneously applied for as many microbial phylotypes as one could imagine. In practice, however, the use of bandpass- , long- and shortpass filters, the use of mercury and/ or argon illumination sources with fixed excitation wavelengths, and the excitation crosstalk of fluorophores dramatically limits the number of fluorophores that can be applied simultaneously in the same experiment **(Waters, 2009)**. Thus, in the past, researchers were mainly limited to 3 different taxa that could be investigated at the same time.

One first solution to this issue was introduced by Amann and colleagues in 1996, where they applied three probes targeted to three sites with little evolutionary conservation of a retrieved rDNA clone, each conjugated to a different fluorochrome. After hybridization, the probes were analyzed using different excitation wavelengths and filter sets, individually recorded and finally superimposed. Each cell could then be visualized according to an additive colour Table, distinguishing up to seven different groups **(Amann et al., 1996)**.

Thanks to the recent advances in fluorescence image acquisition and the application of linear unmixing algorithms to spectrally recorded image data, it is possible to unambiguously identify fluorochromes with overlapping spectra even within the same pixel in a digitally recorded image **(Dickinson et al.,2001; Garini et al., 2006)**. In 2011, a quite extensive but elegant protocol was developed that is based on a linear unmixing algorithm and was applied to a set of 8 binary combinations of probe-dye constructs. They either used two different probes with equal specificity bound to two different fluorophores, or the same probe in two differently labelled versions. After linear unmixing, multichannel images were generated in which each channel consisted of fluorescence intensities assigned to one of the eight fluorophores. The two highest-intensity fluorochromes were then identified, revealing a binary labelling referred to as “label type”. By applying this technique, known as CLASI-FISH (Combinatorial Labeling and Spectral Imaging), 28 different microbial taxa could be visualized simultaneously **(Valm et al., 2011)**.

In another study, Behnam and co-workers developed a new, straightforward DOPE-FISH (double labelling of oligonucleotide probes) approach where each probe was conjugated to two different fluorophores on the 3', and the 5' end **(Behnam et.al, 2012)**. Although this approach completely erases the issue of signal reductions due to the competition of two probes for the same target site, signal reduction might still occur due to quenching effects between the fluorophores due to their close vicinity to each other.

Most recently another study **(Schimak et al., 2016)** proposed a FISH technique referred to as multilabelled FISH or MiL- FISH. The principle behind this approach is similar to the DOPE approach, with the exception that in addition to single and binary combinations, also trinary (in this case fluorescein, Cy5 and Cy3) combinations were used. Signals were recorded separately and subsequently superimposed, resulting in defined, mixed colours that enabled visualization of up to 7 different taxa.

However, as aforementioned, due to intrinsic limitations of microscopes (fixed excitation wavelengths, fixed filters and detectors) researchers in the past were usually constrained to the simultaneous use of three different fluorophores or dependent on combinatorial labelling techniques in order to raise the number of targets per experiment. But owing to the massive improvement of confocal laser scanning microscopy (CLSM) technology in the recent years, this now opens completely new possibilities.

1.2. CONFOCAL LASER SCANNING MICROSCOPY

Objects that are self- luminous solely because of their high temperature are said to emit incandescence. All other forms of light emission are called luminescence. The phenomenon of fluorescence is characterized by molecules, which after the absorption of an appropriate wavelength, emit light for a very short period of time. Compounds that exhibit fluorescence are called fluorophores or fluorochromes and usually emit light when leaving the excited state and returning to lower energy states **(Ploem, 1999)**.

The output of conventional lasers is usually comprised out of one single colour, whereat the bandwidth of the emission is a fraction of a nanometer. This is the reason why the band is called "laser line". Although some lasers (e.g. argon gas lasers) can emit multiple lines in the blue range, in order to excite a set of fluorophores, a set of different laser instruments is needed. These multi-laser systems are composed of a set of lasers and a cascade of beam-combining, semi-transparent mirrors referred to as "laser battery", which has been the workhorse for decades in confocal microscopy. However, the major drawback of these batteries is the fixed excitation wavelengths with no means at all to tune them **(Borlinghaus & Kuschel, 2012)**.

1.2.1. THE WHITE LIGHT LASER (WLL): "BROAD AS A LAMP & BRIGHT AS A LASER"

Very high energy densities in light beams cause several nonlinear effects that alter the properties of the light. In optical fibers these effects are even more pronounced with the strongest effect being found in so called "photonic crystal fibers"- hollow pipes arranged in honeycomb patterns (Figure 1a).

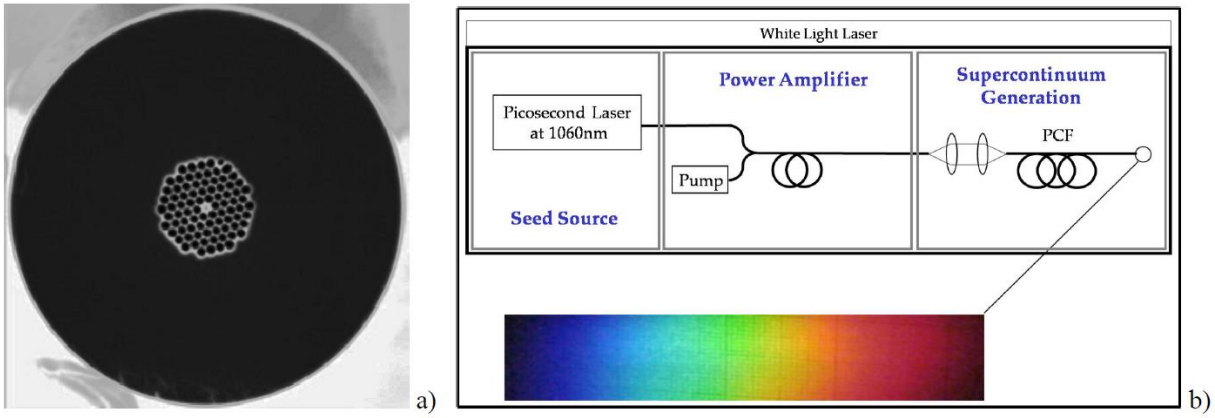

Figure 1 a.) Cross section of a photonic crystal fiber. B.) Arrangement of seed-fiber, pump-fiber laser and photonic crystal fiber in a supercontinuum generating a white light laser. Figure is adopted from Borlinghaus & Kuschel, 2012.

Due to massive nonlinear modifications inside the fibers (phase modulation, Raman scattering etc.), a monochromatic input results in a very broad spectrum with a high spatial coherence at the output- generally referred to as "supercontinuum". The white light laser basically is a sequence of a i) seed

laser that precisely generates pulsed high energy infrared (IR) pulses (usually at 1060 nm), a ii) fiber-pump laser that amplifies the signals in order to achieve a supercontinuum generation, and a iii) photonic crystal fiber that processes and transforms the high power pulses it to a very broad spectrum of a few hundreds of nanometers - the white spectrum (Fig. 1b) **(Borlinghaus & Kuschel, 2012)**.

1.2.2. A TUNABLE OPTICAL FILTER: AOTF

A white illumination source needs an appropriate filter device that selects the exact bands that fit the fluorophore's absorption. Originally filters were based on coloured compounds with which the glass was doped, resulting in selective transmission or blockage of a desired band **(Borlinghaus & Kuschel, 2012)**. Figure 2 gives an overview about the four different filters that have been used in the past. However, one major drawback that all conventional filters face, once again is the fixed and invariable band with no chance to tune these specifications.

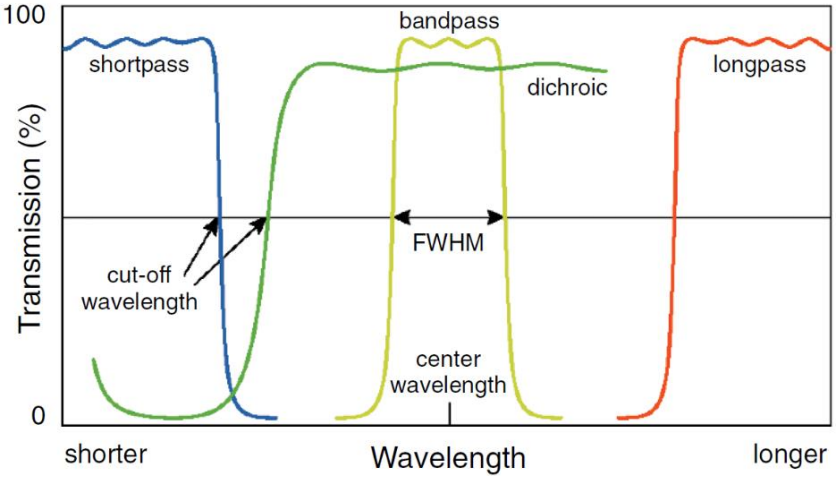

Figure 2: Overview about different types of filters. i) Short- pass filtert cut- off wavelengths longer than a certain wavelength, ii) long- pass filter only transmit light longer than a certain wavelength, iii) bandpass filter only transmit light bewteen a certain treshhold, and iv) dichroic mirrors that operate in a 45° angle, hereby seperating the emitted light from the excitation light (Ploem et al., 1987). Figure is adopted from (Rietdorf & Stelzer, 2006).

The acousto-optical tunable filters (AOTF) use an optical crystal (TeO_2) which is transparent nearly by 100% - 0^{th} order: straight pass. If the crystal is mechanically excited by a standing wave, then a tiny fraction of the white spectrum is directed to a different angle (1^{st} order). This "bandlet" has a width of a couple nm, depending on the respective colour. The colour that is deflected to the 1^{st} order depends on the frequency of the mechanical wave. As the wave is steplessly tunable, one can easily control which colour of the white spectrum exits at 1^{st} order – which in turn is fed into the microscope for extremely specific excitation of any fluorochrome **(Borlinghaus & Kuschel, 2012; Rietdorf & Stelzer, 2006).** Additionally, due to the diffraction properties of an AOTF, precise adjustments can be switched within microseconds **(Harris & Wallace, 1969)** and this device works just as fine for the selection of either a illumination waveband, or a detection band **(Wachman et al., 1997)**.

1.2.3. A TUNABLE BEAM SPLITTER: AOBS

In order to seamlessly carry the desired colours from the laser into the sample an acousto-optical beam-splitter (AOBS) is needed. Basically an AOBS is an AOTF that either combines or separates the light at specific laser wavelengths from all other light **(Rietdorf & Stelzer, 2006)**. The bandlet that is to be picked from the broad spectrum of the WLL can be changed by applying a different mechanical frequency. If the crystal is tuned to a specific wavelength to prime fluorescence in the sample, the excitation light is fed into the 1st order direction. Due to stokes shift, the emitted light is of a different (longer) wavelength and thus will pass straight through the crystal as it is not affected by the diffraction conditions to which the crystal is tuned **(Borlinghaus & Kuschel, 2012; Rietdorf & Stelzer, 2006; Wachman et al., 1997)**.

1.2.4. A TUNABLE SPECTRAL DETECTOR

In order to complete a steplessly tunable detection, a prism and a set of cascaded spectrophotometer slits are used. The slit barriers consist of mirrors that direct a fraction of the spectrum that is not required for the actual detector into different angles to successive detection devices that also have mirrors as barriers which allow operation of further detectors. This concept allows any band to be picked from the white spectrum spanned by the prism in each of the detectors **(Borlinghaus & Kuschel, 2012)**.

1.3. AIM OF THE STUDY

With the just mentioned, massive improvements of the technical key elements that support steplessly tunable excitation and detection of (alternative) fluorophores, and a literally endless choice of the same, the ground is laid for a new, straight-forward multicolour FISH approach that fully exploits the potential of the newest WLL technology.

Thus, the objective of this study is to introduce a new, robust and straight-forward multicolour FISH approach that is based on mono-labelled oligonucleotides and alternative fluorophores. In contrast to previous multicolour approaches that relied on complicated unmixing algorithms **(Valm et al., 2011; Welch et al., 2016)**, or combinatorial labelling techniques **(Amann et al., 1996; Behnam et al., 2012)** that, due to quenching and cross-bleeding effects and different binding affinities of the respective probe-dye construct, are all prone to a certain extend of uncertainty regarding an unambiguous assignment to a certain taxa, this newly introduced technique is expected to be more precise, robust and easy to apply.

Additionally, this method is sought to further deepen a holistic understanding of how complex, microbial community structures are composed, who are the key interacting partners with whom a certain species preferentially interacts, and how this might be interwoven with alterations and adaptations regarding their respective physiology. In other words this ameliorates our understanding of microscale biogeography - the study of the distribution of microbes relative to microscale features of their environment **(Welch et al., 2016)**.

As a proof of principle we aimed to assess and visualize the microdiversity within the nitrifying community of the wastewater treatment plant (WWTP) Ingolstadt, which in the past, has already been extensively investigated **(Gruber-Dorninger et al., 2015)**. What in the past had to be analysed in time-consuming, multiple FISH experiments, now ideally can be achieved in one single FISH experiment. By applying several broad probes targeting all *Bacteria*, AOB and NOB, and a few (sub-) lineage specific NOB probes, we hereby aim to raise the number of microbial taxa that, without any complicated unmixing algorithms or combinatorial labelling, can simultaneously be detected.

2. MATERIAL AND METHODS

The activated sludge samples that were used in this study originate from two different WWTPs. The sludge that is referred to as “Vetmed” was sampled from an aerated, nitrifying activated sludge basin of the full-scale WWTP of the University of Veterinary Medicine, Vienna, Austria in October 2010. The activated sludge that was taken from a sequencing batch reactor at the municipal full-scale WWTP of Ingolstadt, Germany, in March 2011, is referred to as “Ingolstadt”. Samples were immediately fixed upon arrival as described below.

2.1. FISH PROTOCOL

2.1.1. SAMPLE FIXATION

1- 2 ml of sample was centrifuged at 17,949 g for 10 minutes at 4 °C and supernatant was discarded. In order to remove interfering compounds, pellets were resuspended in 2 ml 1x phosphate buffered saline (PBS) and centrifuged as mentioned above. The pellet was then resuspended in 100 µl 1x PBS, quickly vortexed, mixed with 300 µl ice- cold, 3%- PFA solution and incubated at 4 °C for 2 h. Samples then were centrifuged (17,949 g) for 10 minutes at 4°C, supernatant was discarded and the pellet was resuspended in 1 ml 1x PBS and vortexed shortly. After repetition of this washing step, the sample was resuspended in 1 vol. ice- cold 1x PBS, and 1 vol. ice- cold 96% (v/v) ethanol. Fixed biomass was then stored at - 20 °C.

2.1.2. COATING OF MICROSCOPE SLIDES, SAMPLE IMMOBILIZATION & DEHYDRATION

During dehydration, hybridization and washing, biomass often detaches from the plain glass surface of the microscope slide. Thus, in order to improve the adhesion of sample material to the glass surface, slides were agarose-coated. For that purpose, microscope slides were dipped into melted 0.1% (w/v) LE agarose in double distilled water (ddH_2O), subsequently dried applying compressed air and stored at RT. Afterwards, 10 µl of fixed sample were pipetted onto each well and the microscope slides were incubated at 46°C for 15 minutes. Subsequently, in order to permeabilize the cytoplasmic membranes of the target cells and thus making them accessible to oligonucleotide probes, an ascending ethanol series was applied for 3 minutes with 50%, 80% and 96% (v/v) ethanol, respectively. A final drying step at RT completes the dehydration process.

2.1.3. *IN SITU* HYBRIDIZATION

Hybridization buffers with varying respective stringency, were prepared according to Table 1. Formamide (FA) at this juncture interferes with the hydrogen bonds that stabilize nucleic acids duplexes, and thus elevates hybridization stringency. 10 µl of stringent hybridization buffer were applied to each well and mixed with 1 µl of the respective probe working stocks, resulting in a final probe concentration of 0.5 pmol*μl^{-1}. In case multiple probes were applied simultaneously onto the same well, (e.g. five probes requiring 35% FA), hybridization buffers were prepared in a higher FA concentration (70%), that after addition of probes meet the required FA concentration essential for successful hybridization. In order to generate a taut atmosphere, slides were put into a 50 ml screw-top plastic tube harboring a piece of tissue paper that was soaked with the remaining buffer. Screw-top tubes, if not mentioned otherwise, were incubated for 1.5 h in the dark at 46 °C.

Table 1: Composition of different hybridization buffers. Volumes are given in µl.

Formamide (%)	0	5	10	20	25	30	35	40	45	50	70
5M NaCl	180	180	180	180	180	180	180	180	180	180	180
1M Tris/HCl	20	20	20	20	20	20	20	20	20	20	20
ddH_2O	800	750	700	600	550	500	450	400	350	300	100
Formamide	0	50	100	200	250	300	350	400	450	500	700
10% (w/v) SDS	1	1	1	1	1	1	1	1	1	1	1

After hybridization, in order to remove excess probe and formamide, slides were subjected to a 10-minute washing step in the dark at 48°C under stringent conditions. The respective washing buffers were prepared according to Table 2, where at stringency in this case was adjusted via NaCl-concentrations. After washing, the slides were shortly dipped into ice-cold ddH_2O to remove remaining salts, dried with compressed air, and either subsequently analyzed at the microscope, or stored in the dark at -20°C.

Table 2: Composition of washing buffers. Volumes, if not stated otherwise, are given in µl.

Formamide (%)	0	5	10	20	25	30	35	40	45	50	70
5M NaCl	9000	6300	4500	2150	1490	1020	700	460	300	180	0
1M Tris/HCl	1000	1000	1000	1000	1000	1000	1000	1000	1000	1000	1000
0.5M EDTA	0	0	0	500	500	500	500	500	500	500	500
ddH_20	50 ml	50 ml	50 ml	50 ml	50 ml	50 ml	50 ml	50 ml	50 ml	50 ml	50 ml

When probes with different requirements regarding their respective formamide concentrations were applied onto the same well, multiple consecutive hybridization steps were performed, whereat probes requiring the highest formamide concentrations were the first ones to hybridize. Remaining probes were applied in descending order with respect to their individual formamide requirements.

2.1.4. DAPI STAINING

In order to double check correct binding of the probe to its target, all samples (except for ATTO 425 and ATTO 430LS) were stained with 4',6- diamidino- 2- phenylindole (DAPI) **(Lübke, 1993)** after FISH. For that purpose, 15 µl DAPI solution (100 ng/ml) were pipetted onto each well, incubated for five minutes in the dark and thoroughly removed with the pipette. Subsequently each well was subjected to two consecutive washing steps using 15 µl ddH_2O.

2.1.6. OLIGONUCLEOTIDE PROBES USED FOR FISH

Table 3 gives an overview about the all the oligonucleotide probes that have been used in this study. If not specifically stated otherwise, hybridization times were met according to the values below. Probes in light blue represent lineage I specific sub-clusters that are restricted to WWTP Ingolstadt, and probes in dark blue correspond to lineage II specific sub-clusters, that have exclusively been tested on WWTP Vetmed.

Table 3: 16S rRNA targeted oligonucleotide probes used for FISH. * nucleotide numbering according to the 16S rRNA sequence of *E. coli* (Brosius et. al., 1981).

Probe	Specifity	Sequence (5'' 3')	Target site*	FA (%)	Minimal hybridization time applied (h)	Ref.
EUB338	Most *Bacteria*	GCT GCC TCC CGT AGG AGT	338-355	0 - 50	1.5	Amann et al., 1990
EUB338II	*Planctomycetales*	GCA GCC ACC CGT AGG TGT	338-355	0 - 50	1.5	Daims et al., 1999
EUB338III	Verrucomicrobia	GCT GCC ACC CGT AGG TGT	338-355	0 - 50	1.5	Daims et al., 1999
NonEUB	-	ACT CCT ACG GGA GGC AGC	338-355	0-60	1.5	Wallner et al., 1993
Ncom1025	*Nitrosomonas communis* cluster	CTC GAT TCC CTT TCG GGC A	1025-1044	35	1.5	Juretschko 2000
NEU	Most halophilic and halo-tolerant *Nitrosomonas* spp.(incl. *N. europaea,*	CCC CTC TGC TGC ACT CTA	653-670	35	1.5	Wagner et al., 1995

CTE	Competitor of NEU (*Comamonas* spp., *Acidovorax* spp., *Hydrogeno- phaga* spp.,	TTC CAT CCC CCT CTG CCG	659-676	-	1.5	Wagner et al., 1995
Cl6a192	*Nitrosomonas oligotropha* lineage (cluster 6a)	CTT TCG ATC CCC TAC TTT CC	192-212	35	1.5	Adamczyk et al., 2003
C- Cl6a192	Competitor of Cl6a192	CTT TCG ATC CCC GAC TTT CC	192-212	-	1.5	Adamczyk et al., 2003
Nso1225	Betaproteobacterial ammonia-oxidizing bacteria	CGC CAT TGT ATT ACG TGT	1224-1243	35	1.5	Mobarry et al., 1996
Ntspa662	Genus *Nitrospirae*	GGA ATT CCG CGC TCC TCT	662-679	35	1.5	Daims et al. 2001
C- Ntspa662	Competitor of probe Ntspa662	GGA ATT CCG CTC TCC TCT	662-679	-	1.5	Daims et al. 2001
Ntspa 712	Phylum *Nitrospirae*	CGC CTT CGC CAC CGG CCT	712-732	50	1.5	Daims et al. 2001
C- Ntspa712	Competitor of probe Ntspa712	CGC CTT CGC CAC CGG TGT	712-732	-	1.5	Daims et al. 2001
Ntspa1431	*Nitrospira* lineage I	TTG GCT TGG GCG ACT TCA	1431-1448	35	1.5	Maixner et al., 2006
Ntspa1151	*Nitrospira* lineage II	TTC TCC TGG GCA GTC TCT CC	1151-1170	35	1.5	Maixner et al., 2006
Ntspa194	*Nitrospira* Cluster Ia	CTC ACA GCA CGG CTT TCC	194-213	25	3	Gruber-Dorninger et al.
Ntspa1131	*Nitrospira* Cluster Ib	GTG CTC GGC TTG ACC CGG	1131-1147	50	3	Gruber-Dorninger et al.
C- Ntspa1131	Competitor of probe Ntspa1131	GTG CTC GGC ATG ACC CGG	1131-1147	-	3	Gruber-Dorninger et al.
Ntspa451	*Nitrospira* Cluster Ig	AGC AGT TAC CTG CCC CAT	451-477	25	3	Gruber-Dorninger et al.
Ntspa1002	*Nitrospira* Cluster Id	GCT TTC ACC CTT CTA CTA	1002-1018	20	3	Gruber-Dorninger et al.
Ntspa1012	*Nitrospira* Cluster Ie	TAC CTC GTC AGG CTT TCA	1012-1028	20	3	Gruber-Dorninger et al.

2.2. CONFOCAL LASER SCANNING MICROSCOPY

Prior to microscopic analysis, hybridized samples were mounted in Citifluor™ AF1 antifading solution and covered with high precision cover glasses (50x 24 mm, ±170 µm). This step ensures optimal pH for probe excitation and emission and prevents the sample from bleaching during image acquisition **(Johnson et al., 1981).**

2.2.1. IMAGE ACQUISITION

Probe- signals were detected separately by confocal laser scanning microscopy **(Wagner et al., 1994)** using the Leica DMI6000 TCS SP8X, which is equipped with a white light laser and a UV laser (diode) for the excitation of DAPI, ATTO 425 and ATTO 430LS. As it is the characteristic of CLSM, illumination and detection of a tiny spot takes place simultaneously. The tiniest spot that can be created by illumination with farfield optical designs in circular optical systems is the Airy diffraction pattern. Usually this boundary condition is fulfilled by a tiny aperture, the pinhole. **(Kumar et al., 2005; Pawley, 2006)**. The pinhole blocks out-of-focus fluorescence from reaching the detector, and as it is the case in this study, the pinhole was set to 1, resulting in a 1 µm thick section in the z- dimension that was detected. Images (1024 x 1024, 200 Hz) were taken with a glycerol objective lens (HC PL APO CS2/ NA 1.3) with a magnification of X63. The frame average was set to 3 and the line average to 2, respectively, resulting in a pixel dwell time of 1.2 µs. Image detection was performed by the Leica HyD™ photodetector and image processing was done using the standard Leica LAS software package. For the false colour assignment, images were exported as TIFF and pseudo-coloured using the GIMP 2.8.16 freeware.

2.2.2. DAIME EVALUATION OF FLUORESCENCE INTENSITIES

In order to infer signal brightness of the newly introduced fluorophores and to compare the relative signal intensities to the most common and brightest dye routinely available, namely the carbocyanine dye Cy®3, the daime software was applied **(Daims et al., 2006)**. For the daime evaluation it is crucial, that all pictures are acquired with the exact same instrument settings (e.g. Laser power, smartgain) **(Daims & Wagner, 2011)**. Thus relevant settings were tuned to values that yielded bright, but not overexposed signals for Cy3 conjugated to the EUBI probe **(Amann & Binder et al., 1990)**. Settings for Cy3 were as follows: Laser power: 20%, pinhole: 1, smart gain: 75% and pixel dwell time: 1.2 µs. These exact same settings were applied to all remaining dyes for image acquisition, biomass was coloured grey and images were exported as TIFF formate without any further manipulations.

To differentiate between background, biomass (microbes) and ambiguous signals (autofluorescent debris), a pre-processing step referred to as “image segmentation” was applied. When necessary, segmentation was manually refined using the “interactive object editor”. Image segmentation is based on the rapid automated threshold selection (RATS) algorithm **(Kittler et al., 1985)**, that identifies biomass based on the brightness of the fluorescence signal **(Daims et al., 2006; Daims & Wagner, 2011)**. Finally, upon analysis, daime calculates the mean intensities of all objects (excluding holes), including several other statistically relevant values (e.g. standard errors of the mean, standard deviation, number of objects etc.). Data were finally exported and analysed using Excel 365 ProPlus.

2.3. ALTERNATIVE FLUOROPHORES

Alternative fluorophores were chosen in order to maximize the number of dyes that can be simultaneously excited with the diode (405 nm) and the white light laser spectra (470-670 nm) and the concurrent intention to keep overlapping emission or excitation spectra of the fluorophores to a minimum (Figure 3, Table 4). A further selection criterion, besides the ability to prime fluorescence in alkaline buffered solutions which was a prerequisite, these dyes are also provided by current companies synthesizing fluorescently labelled oligonucleotides.

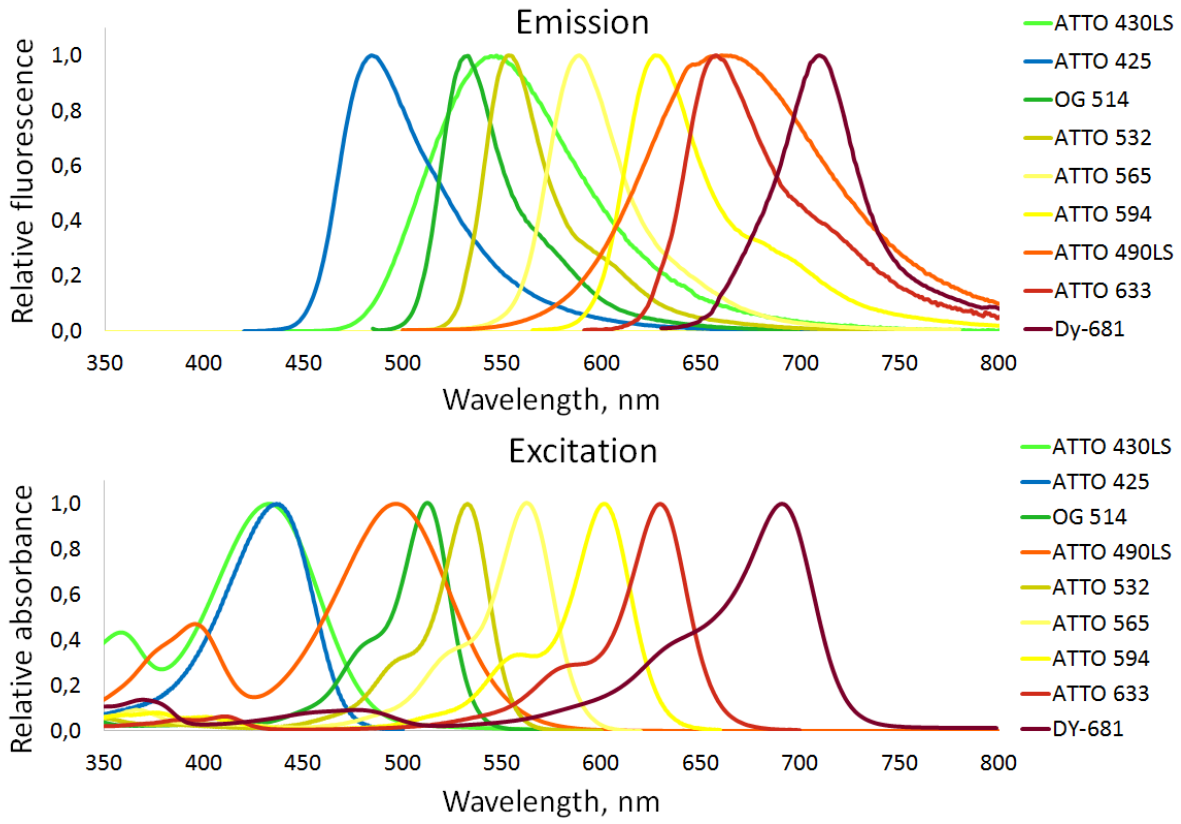

Figure 3: Excitation and emission spectra of all alternative fluorophores applied in this study.

Due to Stokes shift, the emission peaks are usually shifted about 15- 30 nm towards the longer wavelength (Table 4). However, ATTO 425 exhibits a stokes shift of 66 nm, ATTO 430LS of 114 nm and ATTO 490LS even extends this shift to 165 nm, making these 3 fluorochromes theoretically the perfect choice for multicolour FISH. The intrinsic feature of the long shift dyes allowed it for ATTO 430LS and ATTO 490LS to expand the detection to window to 40 nm. For all other dyes the detection window was set to 20 nm.

Since the emission of the diode laser is fixed at 405 nm, it was not possible to excite ATTO 425, nor ATTO 430LS at their excitation maxima (439 nm and 436, respectively). The excitation peak of Dy-681 is with 691 nm also outside of the spectra that is provided by the WLL. Thus Dy-681 was excited as close to the excitation peak as possible, more precisely at 670 nm. All the other dyes were excited as stated below. Cy3, Oregon Green 514 and ATTO 430LS were excluded from multicolour experiments due to crossbleeding or excessive unspecific binding. Cy3 instead was applied for the daime evaluation and to double check and compare signals of specific probes and Fluos was applied for multicolour experiments.

Table 4: Properties of all fluorophores applied in this study. λ_{max} corresponds to absorption, and emission maxima, respectively. ε_{max} depicts the molar extinction coefficient, QY the fluorescence quantum yield in water, DT the decay time, and MW the molecular weight. Highlighted backgrounds state the particular colour that corresponds to the respective wavelengths used for excitation and emission of the desired fluorophore. The detection window defines the spectrum on the CLSM at which the respective emissions were collected. All data obtained from the manufacturer's homepage (atto-tec.com; dyomics.com; sigmaaldrich.com, and as it is the case with Dy-681, from (Pauli et al., 2010)).

Fluorophore	λ max (excitation)	λ max (emission)	Detection window (nm)	ε max [l/mol x cm]	QY (%)	DT (ns)	MW (g/mol)
ATTO 425	439 nm	485 nm	475-495	$4,5 \times 10^4$	90%	3,6	401
ATTO 430LS	436 nm	545 nm	525-565	$3,2x10^4$	65%	4,0	589
ATTO 490LS	496 nm	661 nm	645-685	$4,0 \times 10^4$	30%	2,6	696
ATTO 532	532 nm	552 nm	545-565	$1,15 \times 10^5$	90%	3,8	765
OG 514	513 nm	533 nm	520-540	N/A	N/A	N/A	609
ATTO 565	564 nm	590 nm	580-600	$1,2 \times 10^5$	90%	4,0	611
ATTO 594	603nm	626 nm	620-640	$1,2 \times 10^5$	85%	3,9	1137
ATTO 633	630 nm	651 nm	650-670	$1,3 \times 10^5$	64%	3,3	652
Dy-681	691 nm	708 nm	700-720	$1,4 \times 10^5$	11%	N/A	737
FLUOS	492 nm	517 nm	510-530	7×10^4	N/A	N/A	473
Cy3	554 nm	668 nm	550-570	$1,5 \times 10^5$	15 %	N/A	767

Table 5 gives and overview about the probe-dye combinations that have been used for the multicolour FISH experiments. The first (50% FA) and the second (35% FA) hybridization could be managed within one day. Slides were then frozen away over night at -20°C and the third hybridization (25% FA) was carried out. To overcome the dim signals of Ntspa194 and Ntspa451, probes were double labelled.

Table 5: Probes and dyes used for the multicolour FISH approach. FA = formamide.

Probe	Fluorophore	Excitation	Emission	Target	FA	Hybridization time (h)
Ntspa 1131	ATTO 532	532	545-565	Lin 1b	50%	3
EUB mix	ATTO 425	405	475-495	EUB	35%	1.5
AOB mix	FLUOS	492	510-530	AOB	35%	1.5
NOB mix	ATTO 490LS	496	645-685	NOB	35%	1.5
Ntspa 1151	DY-681	670	700-720	Lin II	35%	1.5
Ntspa 1431	ATTO 565	564	580-600	Lin I	35%	1.5
Ntspa 194	ATTO 633 DOPE	630	650-670	Lin 1a	25%	3
Ntspa 451	ATTO 594 DOPE	601	620-640	Lin 1g	25%	3

3. RESULTS

4.1. SINGLE EVALUATION OF ALTERNATIVE FLUOROPHORES

In order to evaluate the general *in situ* suitability of the newly introduced fluorophores, dyes were conjugated to EUB and NON probes and applied on activated sludge samples from the WWTP Ingolstadt. All samples (except for ATTO 425 and ATTO 430LS) were DAPI stained (Fig. 5-11) to additionally verify signals with a well-established fluorescent dye and for the two dyes that were excited with the diode, transmission was used instead of DAPI to avoid interference of the same with the fluorophores (Fig. 4).

Of the initial nine alternative fluorophores, eight exhibited sufficiently bright and clear signals (Fig. 4-11). For ATTO 430LS it was not possible to unambiguously distinguish between the EUB and the NON probe (Fig. 4: C, D). ATTO 425 also yielded relatively strong fluorescence when conjugated to the nonsense probe (Fig 4: B), but EUB signals were significantly stronger and thus remained distinguishable from unspecific binding or autofluorescence.

ATTO 425 (instead of DAPI) was solely applied to visualize biomass in general and thus this dye was only conjugated to the EUB and the NON probe. All remaining dyes were additionally bound to various specific probes targeting different microbial taxa of the nitrifying community present in the activated sludge samples from WWTP Ingolstadt and WWTP Vetmed. Samples were again DAPI stained to visualize all cells and specific probes were additionally applied in Cy3 in order to double check and compare signals (Fig 5-11, C, D).

OG 514 mostly yielded clear signals during pre-evaluations (Fig 6), but unspecific binding could be observed more frequently then with other alternative fluorophores. As Fluos (in regard to the excitation and emission wavelengths) has similar properties as OG 514, but showed a more stable performance and additionally is cheaper than OG 514 (at Biomers), we decide to continue to use this conventional fluorophore for the multicolour FISH approach, and thus also excluded OG 514 from all further experiments and evaluations.

Owing to the very big cell-clusters and flocs in activated sludge, both used sludge samples exhibited a very strong intrinsic 3D-topology. The activated sludge retrieved from WWTP Vetmed featured a higher tendency for unspecific binding and depositions of probe-dye conjunctions than samples retrieved from Ingolstadt. The reoccurring effect of depositions was especially pronounced for the Ntspa1012 probe conjugated to ATTO 594, a sub-cluster of lineage II *Nitrospira* exclusively found in

WWTP Vetmed. Due to the many depositions it was not possible to unambiguously distinguish specific signals from the nonsense probes and thus further single evaluations of specific probes were tested on Ingolstadt.

Single evaluation of specific probes on Ingolstadt resulted in clearly discriminable signals (Fig. 5-11), regardless whether relatively broad (AOB, NOB, lineage I and lineage II *Nitrospira*), or highly specific probes (sub-clusters of lineage I *Nitrospira)* were used.

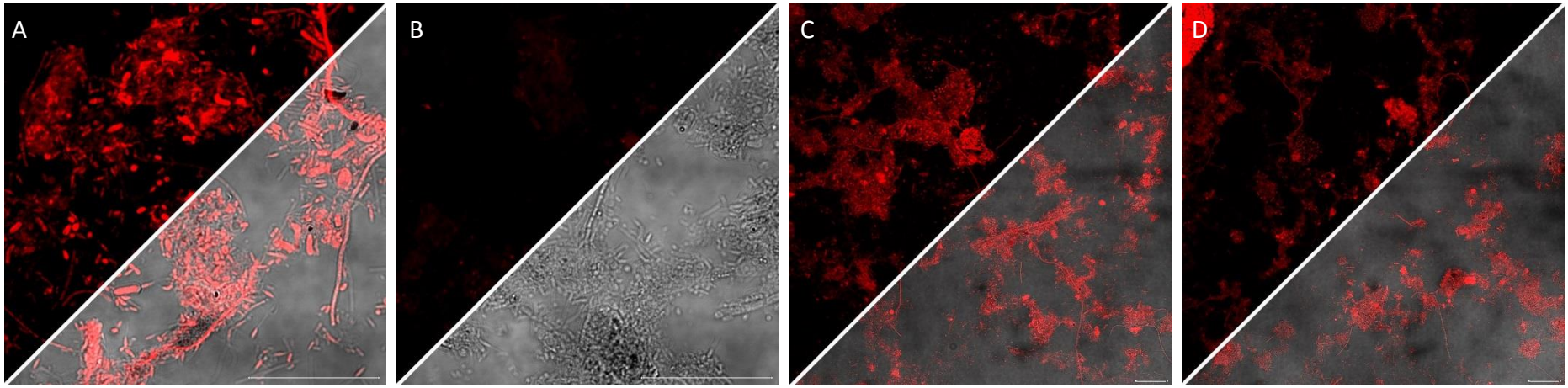

Figure 4: Single evaluation of ATTO 425 (A, B) and ATTO 430LS (C, D). A and C depict EUB probes conjugated to ATTO 425 and ATTO 430LS, respectively. B and D represent the respective NON probes. Image acquisition settings for ATTO 425 were: LP= 5%, SG= 120%, P= 1. Settings for ATTO 430LS were: LP= 8%, SG= 100%, P= 1. Scale bar depicts 20 µm.

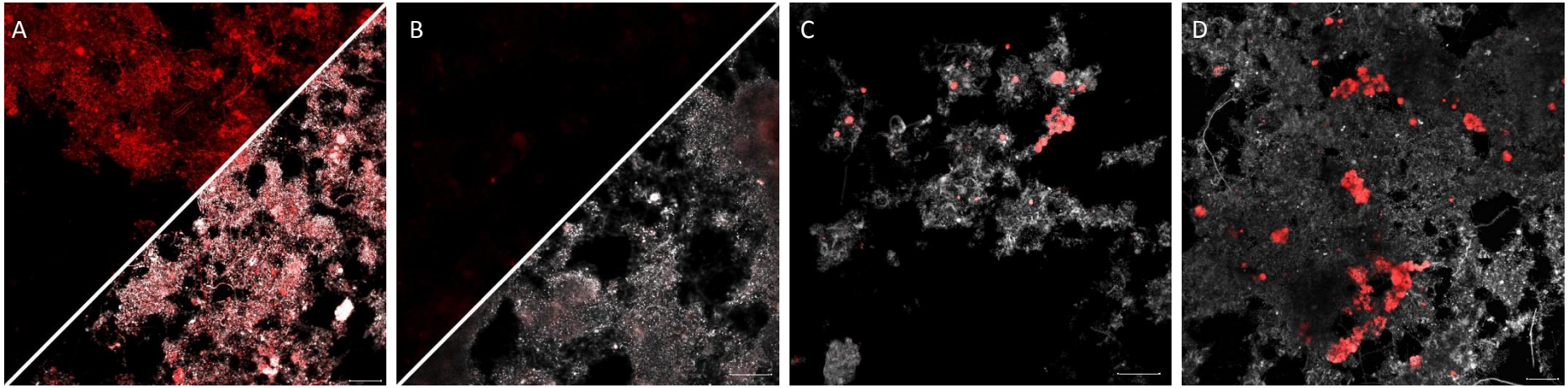

Figure 5: Single evaluation of ATTO 490LS. A and B depict EUB and NON probes and highlighted clusters represent NOB colonies targeted by the NOB-mix in ATTO 490LS (C) and Cy3 (D). Image acquisition settings for ATTO 490LS were: LP= 30%, SG = 100%, P= 1. Settings for Cy3 were: LP= 30%, SG= 15%, P= 1. Scale bar depicts 20 µm.

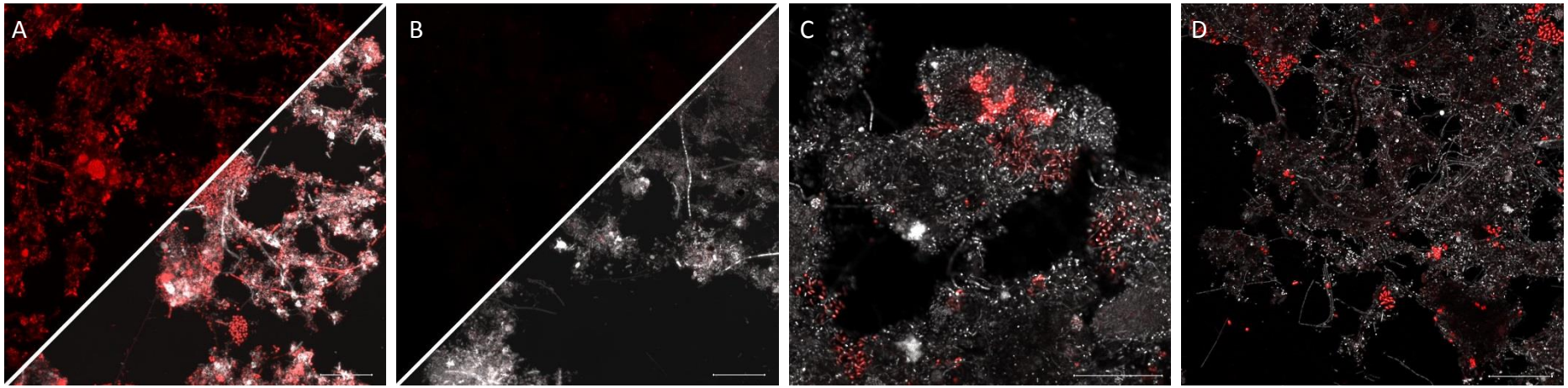

Figure 6: Single evaluation of Oregon Green 514. A and B represent EUB and NON probes. Red cells represent AOB colonies targeted by the AOB-mix in OG 514 (C) and Cy3 (D), respectively. Image acquisition settings for OG514 were: LP= 30%, SG= 200%, P= 1. Settings for Cy3 were: LP= 30%, SG= 30%, P=1. Scale bar depicts 20 µm.

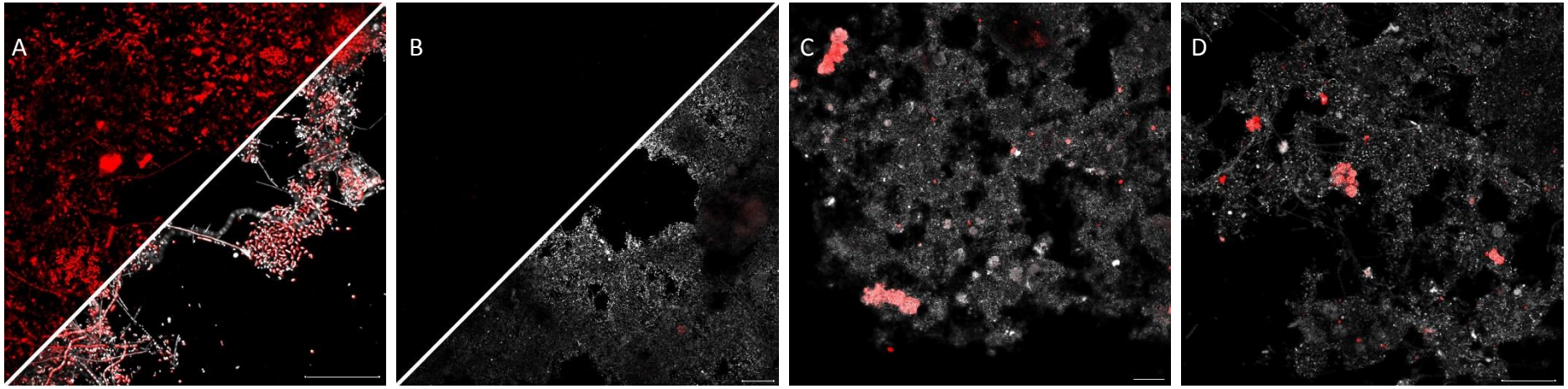

Figure 7: Single evaluation of ATTO 532. A and B represent EUB and NON probes. Red cauliflower-shaped colonies represent *Nitrospira* affiliated with lineage I targeted by the Ntspa1431 probe conjugated to ATTO 532 (C) and Cy3 (D), respectively. Image acquisition settings for ATTO 532 were: LP= 20%, SG= 150%, P= 1. Settings for Cy3 were: LP= 20%, SG= 85%, P=1. Scale bar depicts 20 µm.

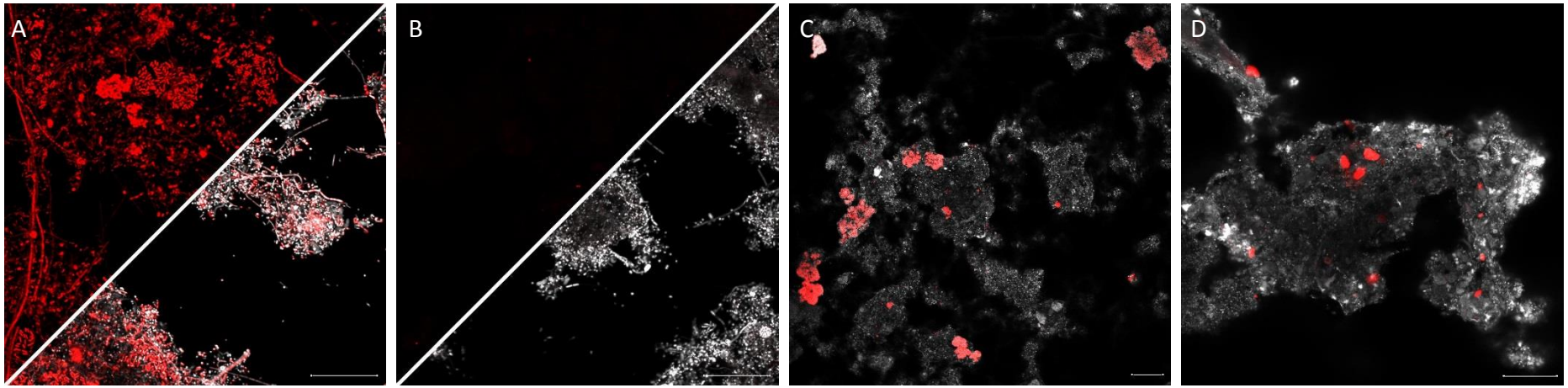

Figure 8: Single evaluation of ATTO 565. A and B represent EUB and NON probes. Red cauliflower-shaped colonies represent *Nitrospira* affiliated with lineage I targeted by the Ntspa1431 probe conjugated to ATTO 565 (C) and Cy3 (D), respectively. Image acquisition settings for ATTO 565 were: LP= 10%, SG= 80%, P= 1. Settings for Cy3 were: LP= 10%, SG= 80%, P=1. Scale bar depicts 20 µm.

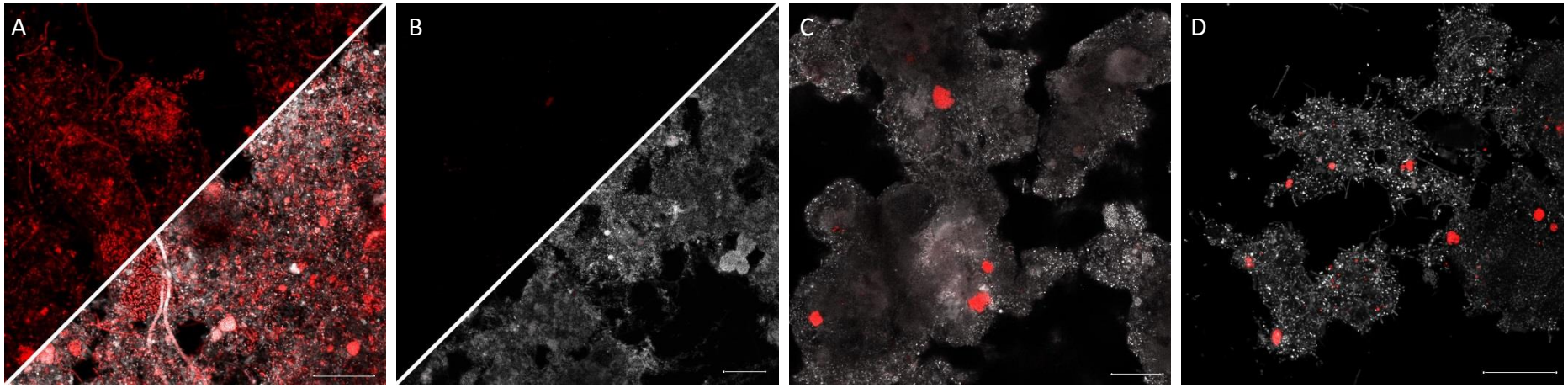

Figure 9: Single evaluation of ATTO 594. A and B represent EUB and NON probes. Highlighted spherical clusters represent *Nitrospira* affiliated with sublineage Ig targeted by the Ntspa451 probe conjugated to ATTO 594 (C) and Cy3 (D), respectively. Image acquisition settings for ATTO 594 were: LP= 10%, SG= 100%, P= 1. Settings for Cy3 were: LP= 10%, SG= 45%, P=1. Scale bar depicts 20 µm.

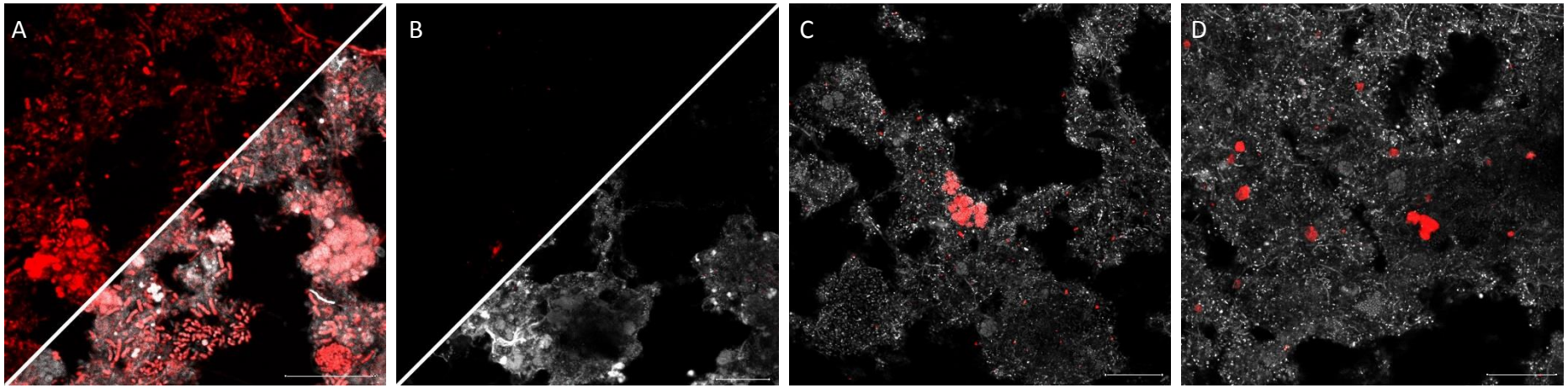

Figure 10: Single evaluation of ATTO 633. A and B represent EUB and NON probes. Highlighted, irregularly shaped clusters represent *Nitrospira* affiliated with sublineage Ia targeted by the Ntspa194 probe conjugated to ATTO 633 (C) and Cy3 (D), respectively. Image acquisition settings for ATTO 633 were: LP= 15%, SG= 100%, P= 1. Settings for Cy3 were: LP= 10%, SG= 45%, P=1. Scale bar depicts 20 µm.

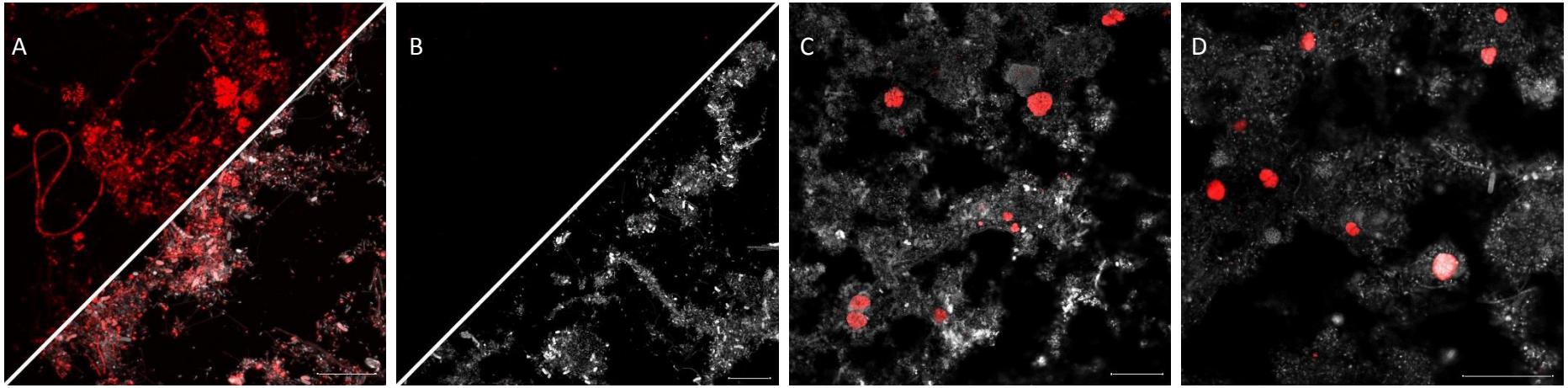

Figure 11: Single evaluation of Dy-681. A and B represent EUB and NON probes. Highlighted spherical colonies represent *Nitrospira* affiliated with lineage II targeted by the Ntspa1151 probe conjugated to Dy-681 (C) and Cy3 (D), respectively. Image acquisition settings for Dy- 681 were: LP= 20%, SG= 120%, P= 1. Settings for Cy3 were: LP= 20%, SG= 30%, P=1. Scale bar depicts 20 µm.

4.2. DAIME EVALUATION OF MEAN FLUORESCENCE INTENSITIES

Boxplots are a convenient and robust way of graphically depicting groups of numerical data through quartiles, making them ideal for showing overall patterns of a response for a certain group **(Fahrmeir et al., 2007)**. To compare the *in situ* signal intensities of alternative fluorophores to Cy3, dyes were conjugated to EUB probes and applied on activated sludge samples retrieved from the WWTP Ingolstadt. The two dyes that are excited at 405 nm (ATTO 425, ATTO 430LS) could not be considered in this measurement because the light that was used for excitation originates from the diode rather than from the WLL and thus intensities are not directly comparable.

Figure 12 visualizes the respective signal brightness of each dye relative to each other and Table 6 depicts the exact corresponding values according to the daime output. Counted objects varied between 322 (ATTO 633) and 748 (ATTO 490LS), maximum relative fluorescent values between 88 (ATTO 565) and 24 (Dy-681) and minimum fluorescent values between 17 (ATTO 633) and 5 (ATTO 490LS).

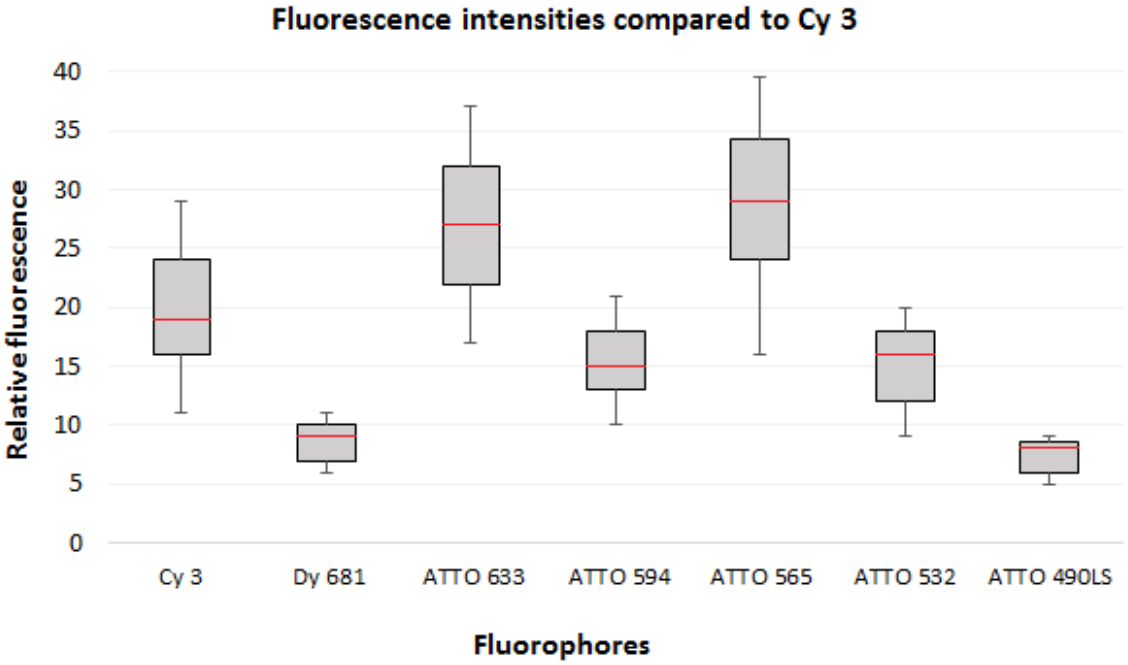

Figure 12: Boxplot diagram of measured signal intensities of all alternative fluorophores applied in the multicolour approach. Red line depicts the median, boxes represent the interquartile range (IQR) and whiskers represent the respective maxima and minima values.

Generally speaking, the variance is highest for the three brightest dyes (Cy3, ATTO 633, ATTO 565), already declining for dyes exhibiting an intermediate signal brightness (ATTO 594, ATTO 532) and very little for the dimmest dyes Dy-681 and ATTO 490LS, respectively.

The interquartile range (IQR) harbours 50% of all measured values and therefore depicts a very robust part for direct comparison. As shown above, ATTO 633 and ATTO 565 turned out to be much brighter than Cy3 with ATTO 633 showing only a very narrow overlay with Cy3, and ATTO 565 showing no overlay at all (Fig. 4).

The fluorophore brightness or the fluorescence output per fluorophore is proportional to the product of the molar extinction coefficient and the fluorescent quantum yield. The respective theoretical and expected values are given in Table 6. Since the objective of this measurement was to assess the brightness of alternative fluorophores relative to Cy3, the brightness of the carbocyanine dye per definition is 100%. All other values are given in percentages relative to Cy3. According to the theoretical, calculated brightness four fluorophores should (by far) exceed the signal brightness of Cy3. However, experimental data showed that in practice only ATTO 633 and ATTO 565, with a relative brightness of 145% and 155%, respectively, seem to be superior to Cy3. ATTO 594 and ATTO 532 on the contrary, in each case only yielded 80% relative fluorescence, lagging behind the theoretical value by a factor of 5.7 and 5.8, respectively. Also the dimmest dyes Dy-681 (45%) and ATTO 490LS (40%) lag behind their theoretical values, albeit the discrepancy between theoretical and experimentally assessed values is less pronounced than for all the other dyes.

Table 6: Measured fluorescence intensity values according to daime. Std. dev. represents the standard deviation, Std. err. the standard error and n the number of counted objects, respectively. Expected brightness was calculated according the the QY- and εmax values stated in Table 4. Measured brightness refers to the mean intensity values calculated by daime.

	Cy3®	Dy-681	ATTO 633	ATTO 594	ATTO 565	ATTO 532	ATTO 490LS
Minimum.	11	6	17	10	16	9	5
Mean	20	9	29	16	31	16	8
Maximum	62	24	76	38	88	37	33
Median	19	9	27	15	29	14	8
Std. dev.	7	3	9	5	10	5	2
Std. err.	0	0	1	0	0	0	0
n	390	650	322	395	518	450	748
Expected brightness	100 %	68 %	370 %	453 %	480 %	460 %	53 %
Measured brightness	100 %	45 %	145 %	80 %	155 %	80 %	40 %
Decrease by a factor of	-	1.5	2.6	5.7	3.1	5.8	1.3

4.3. PROOF OF PRINCIPLE: MULTICOLOUR FISH

In order to proof the applicability of this new multicolour FISH concept on activated sludge samples, the already previously well described microdiversity of *Nitrospira* occurring in the WWTP Ingolstadt was visualized **(Gruber-Dorninger et al., 2015)**. To achieve a simultaneous visualization of all targeted subpopulations, three consecutive hybridization steps with varying FA concentration were carried out. The 3rd hybridization was only carried out when the previous hybridizations seemed promising. As shown in Figures 14-16, simultaneous detection of six different microbial guilds within one field of view was achieved. Moreover, it was possible to verify and visualize the presence of all three lineage I *Nitrospira*-specific sub-clusters, whose occurrence has already been stated in a previous study **(Gruber-Dorninger et al., 2015)**. As we could apply a whole set of additional fluorophores, it not only was possible to simply verify the presence of a certain microbial (sub-)cluster, but also to visualize the spatial arrangement of the same relative to other microbial players participating in nitrification.

As illustrated in Figure 13, autofluorescence of the activated sludge sample generally was very weak and did not cause interference with image acquisition. Only channels tuned to the detection of ATTO 425, ATTO 490LS and ATTO 532 exhibited slight autofluorescence, and this effect was most pronounced for ATTO 532.

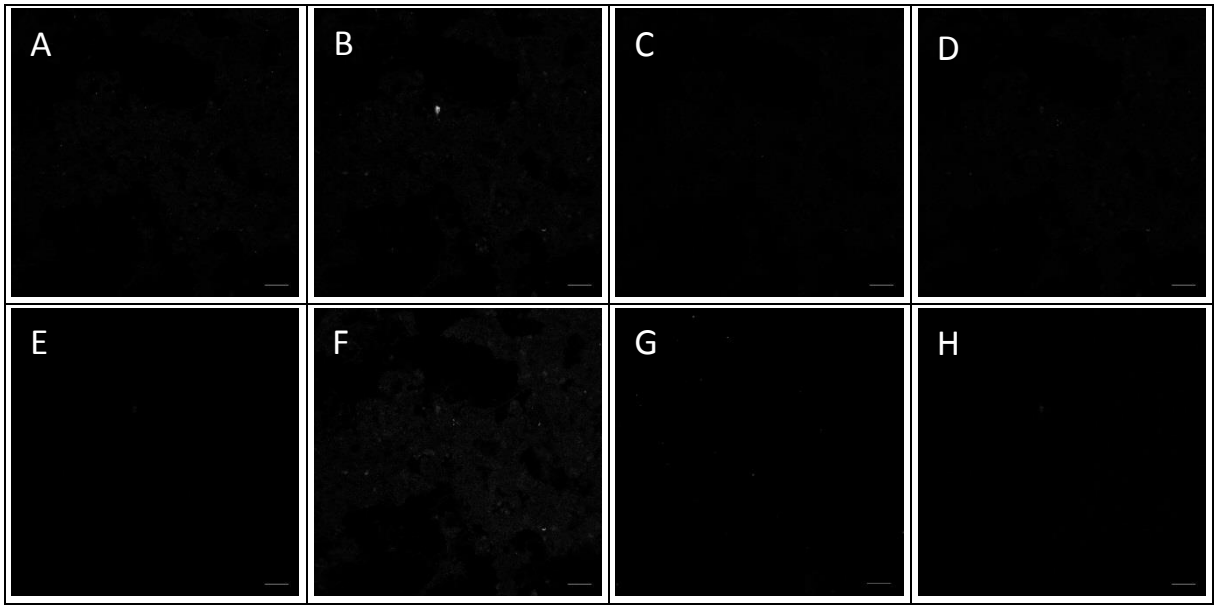

Figure 13: Autofluorescence of an unhybridized sludge sample from the WWTP Ingolstadt. Channels were individually recorded, whereat A= ATTO 425, B= ATTO 490LS, C= Fluos, D= ATTO 565, E= Dy-681, F= ATTO 532, G= ATTO 594, H= ATTO 633. Scale bar depicts 20 µm.

Since all (except bacteria targeted solely by the EUB probe) microbial clusters were not only targeted by one single probe, but rather by up to four probes, Table 7 depicts the false colour assignment for each unique probe combination targeting a certain group.

Table 7: Additive probe Table that itemizes all probes targeting a certain colony and the corresponding false colour assignment.

	Gray	Green	Cyan	Purple	Red	Orange	Blue	Yellow[1]	Green[2]
Target	EUB	EUB	EUB	EUB	EUB	EUB	EUB	EUB	EUB
Target		AOB	NOB	NOB	NOB	NOB	NOB	NOB	NOB
Target				lineage II *Nitrospira*	lineage I *Nitrospira*	lineage I *Nitrospira*	lineage I *Nitrospira*	Sub-cluster Ib	Sub-cluster Ig
Target						Sub-cluster Ib	Sub-cluster Ia		

[1]Sub-clusters (except for sub-cluster Ig) are also targeted by the lineage I *Nitrospira* specific probe. However, hybridization with the given probe was not successful in the experiment depicted in Figure 16.

[2]Green pseudo-colouring marked with [2] is exclusively valid for Figure 16.

The probe Ntspa 1131 (ATTO 532) was the only one to be hybridized in the 1st step, with 50% formamide in the hybridization buffer. After the first hybridization, the Ntspa1131 probe showed bright and very clear signals in all attempts. However, after the 2nd hybridization step signal intensities

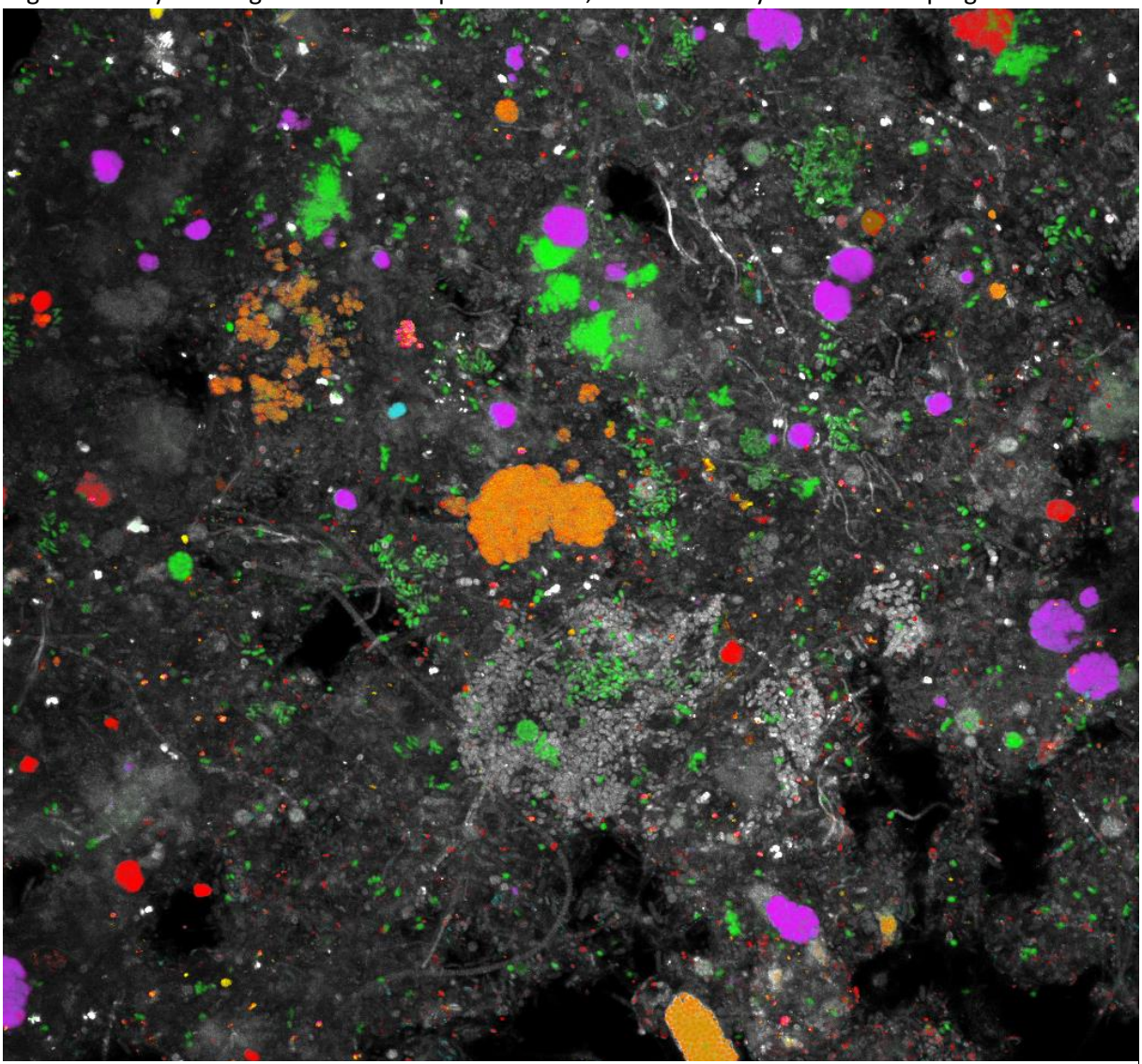

Figure 14: The pinhole was set to 1 for all dyes, laser power (LP) and smart gain (SG) were as follows: ATTO 425: LP= 10, SG= 70; ATTO 490LS: LP=20, SG=200; Fluos: LP= 25, SG= 200; ATTO 565: LP= 20, SG= 120; Dy- 681: LP= 20, SG= 100; ATTO 532: LP= 20, SG= 200.

generally were already massively decreased or completely washed off. Especially the big, irregularly cauliflower-like shaped clusters (Fig. 16c) were prone to signal fading more strongly than the rather small and squat clusters. This effect was further pronounced after the 3rd hybridization, where clear signals (of small colonies) could only be obtained sporadically after a long time of searching.

The second hybridization performed at 35% FA included probes targeting the AOB (here applied in Fluos) and caused issues by either not being detectable at all, or by ambiguous binding motifs (e.g. binding to colonies that clearly were NOB). When hybridization was successful, AOB colonies usually were found as loose cells embedded in the matrix of the activated sludge, but also as tight, irregularly and spherically shaped united cell structures (Fig. 14, 15).

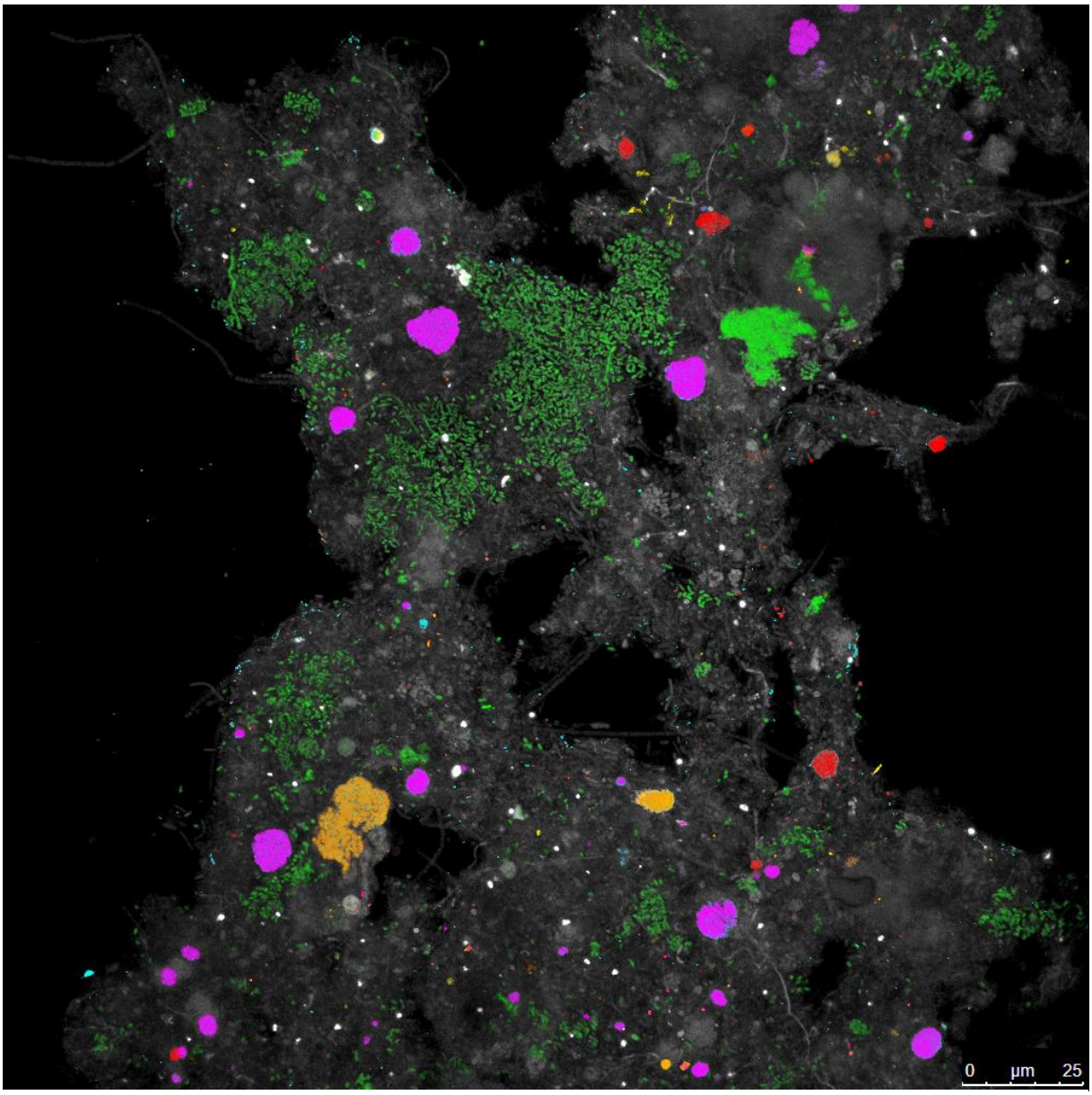

Figure 15: The pinhole was set to 1 for all dyes, LP and SG were as follows: ATTO 425: LP= 10, SG= 70; ATTO 490LS: LP=20, SG=200; Fluos: LP= 25, SG= 200; ATTO 565: LP= 20, SG= 120; Dy- 681: LP= 20, SG= 100; ATTO 532: LP= 20, SG= 200.

The EUB probe (ATTO 425), the Ntspa1151 probe (Dy-681/ ATTO 565) targeting lineage II *Nitrospira* as well as the probes comprising the NOB-mix (ATTO 490LS) worked throughout every single experiment. Though ATTO 490LS is a rather weak fluorescent dye and signals usually were much dimmer in comparison to other dyes, signals always were clearly discriminable and highly specific, even after the 3rd hybridization. Clusters captured by the lineage II probe were almost exclusively of typical, tight and spherical shape strongly resembling cauliflowers, with only sporadic bigger and loose clusters as shown in Figure 16a.

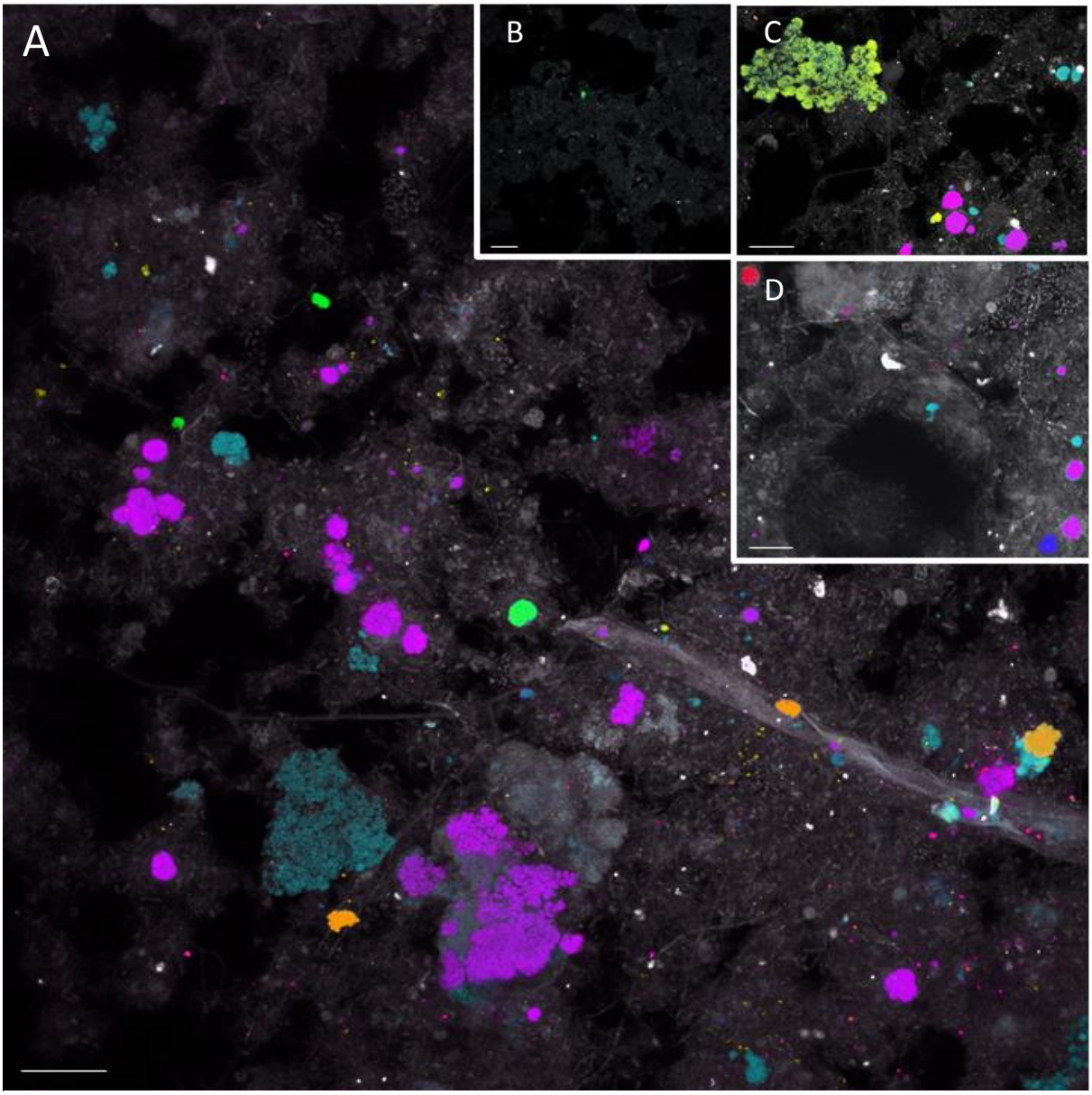

Figure 16: B illustrates autofluorescence of the activated slude sample when all eight channels are recorded on an unhybridized sludge sample. The pinhole was set to 1 for all dyes, LP and SG were as follows: ATTO 425: LP= 10, SG= 70; ATTO 490LS: LP= 30, SG= 200; ATTO 565: LP= 30, SG= 180; Dy- 681: LP= 20, SG= 100; ATTO 532: LP= 20, SG= 200; ATTO 594: LP= 10, SG= 80; ATTO 633: LP= 20, SG= 90.

In the 3rd hybridization, two double labelled, lineage I *Nitrospira* specific probes targeting the sub-cluster Ia (ATTO 633) and sub-cluster Ig (ATTO 594), respectively, were hybridized at 25% FA (Figure 16 A, D). Here, we chose a double labelling strategy based on the fact that also in the original study these

probes needed to be double labelled to prime sufficient fluorescence **(Gruber-Dorninger et al., 2015)**. After the 3rd hybridization, signals obtained from Ntspa1131 (1st hybridization), Ntspa1431, AOB- and NOB-mix (2nd hybridization), were relatively weak, of reduced specificity or utterly missing. This issue could be counteracted by raising the probe concentration from 5 to 10 pmol which perceptibly ameliorated this obstacle. The DOPE-labelled probe Ntspa451 (ATTO 594) targeting sublineage Ig *Nitrospira* could be assessed very clearly showing distinct signals without any unspecific binding (Fig. 16a). The sublineage Ia (ATTO 633, DOPE) featured relatively strong depositions and clear visualization only worked for small colonies (Fig. 16d). Due to time limitations this issue could not be further ameliorated. However, when applied in a single experiment both probe-dye combinations featured very bright and clearly distinguishable signals, whereat the clusters targeted by the Ntspa451 probe always were of small, tight and round shape in contrast to clusters targeted by Ntspa194, that also included very big, irregularly cauliflower-shaped colonies similar to those targeted by Ntspa1131.

4. DISCUSSION

4.1. SINGLE EVALUATION OF ALTERNATIVE FLUOROPHORES

The rationality behind the appliance of Cy3 for brightness comparisons and signal double checking is self-evident, as this dye has been the workhorse for many FISH applications in the last 20 years. Reasons for the great popularity amongst scientists are a remarkably high stability against photobleaching, compatibility with commonly available lasers that emit in the green spectra, commercial availability **(Sanborn et al. 2007)** and the fact, that it has been the brightest dye available for quite some time **(Wessendorf & Brelje, 1992)**.

As depicted in Figure 4 C & D, it was not possible for ATTO 430LS to clearly distinguish the EUB-probe conferred signals from those of the nonsense probe. Also, correction attempts (e.g. the adjustment of contrast and/ or brightness and laser power) did not result in a clearer and unambiguous discrimination between the EUB and NON probe. One reason that could explain this issue is the fact, that ATTO 430LS (due to the fixed excitation wavelength of the diode) could not be excited at the excitation maxima. Thus one needs more laser power to excite the dye to a certain extent, as if it would be feasible by the excitation at the maxima peak. Consequently, with an increased intensity of the laser beam exciting the sample, also excessive dye remnants that were not washed off and/or depositions carry more weight and autofluorescence increases. Another study dealing with ATTO 430LS also reported that UV light that is used for excitation often is incompatible with imaging of biological samples **(Maksim, 2015).** Though the wavelengths used for excitation (405 nm) is already within the visible spectra, it nevertheless is relatively close to the UV- spectra and thus this might also have an impact.

A similar effect (albeit less pronounced) could also be observed for ATTO 425 (Fig. 5 A, B), another dye that was excited with the diode (below its excitation maxima). However, after adjustment of laser power and/or the same tuning of contrast and brightness for EUB and NON-EUB images, a clear distinction with regard to fluorescence brightness between EUB and the NON-EUB image could be obtained. As in our case ATTO 425 solely was used to visualize and thus differentiate the biomass from the background rather than screening for specific microbial guilds or clusters, this clear but rather weak difference was sufficient. Whether or not one might use this dye conjugated to specific probes constitutes a question that needs to further be tested.

All the other dyes yielded very promising and clear results with regard to the EUB/NON comparison and also the varying specific probes (Fig. 6-12). Further, all dyes that were excited with the WLL seem to be perfectly compatible for FISH applications as during the single evaluation they neither were prone to unspecific binding, nor to excessive depositions or photobleaching.

4.2. DAIME EVALUATION OF MEAN FLUORESCENCE INTENSITIES

Fluorophores suitable for FISH and similar visualization approaches applied in the fields of microbiology and cell biology should adsorb and emit within the desired window of the visible spectra with a high molar absorption coefficient (ε) at the excitation wavelength and a high fluorescent quantum yield (Φf) under experimentally relevant conditions. Furthermore, the fluorophores should exhibit a high photochemical stability, good solubility in aqueous solutions, low unspecific binding and a rapid and preferable complete clearance of the free dye after washing **(Licha, 2002)**. Although these requirements are theoretically met by all the newly introduced fluorophores, pronounced discrepancies between calculated and experimentally observed brightness were determined with only two out of four fluorophores actually exceeding the measured brightness of Cy3 (Fig. 12, Table 6).

These deviations between theory and practice can be addressed to several different factors influencing the quantum yield, and thus finally the fluorophore's brightness. **Raghavachari (2000)** could show that conformational changes of the fluorophore that might appear in form of cis-trans isomerization in the excited state, displays a major source of non-radiative energy transfer. Another factor reducing the quantum yield depicts the formation of non-fluorescent aggregates (dimerization) **(Philip et al., 1996; Raghavachari, 2000)**, which is affected by dye charge and hydrophilicity **(Philip et al., 1996)**.

Fonin and colleagues (2014), amongst other factors, further linked the issue of reduced fluorescence intensity to the secondary inner filter effect. This effect is characterized by self-quenching of the dye that is due to an overlap of the excitation and emission spectra. Additionally the formation of excimers (dimers, where one dye molecule is found in the excited state, the other one resides in the ground state) and collision of excited fluorophores with those lingering in the ground state, are known to decrease fluorescence intensity **(Fonin et al., 2014)**.

In the past it could also be shown, that the fluorescence intensity of the carbocyanine dye Cy3 is bonding dependent. The quantum yield was highest when attached to the 5' terminus of single stranded DNA (ssDNA) and decreased by a factor of 2.4 when double stranded DNA (dsDNA) was formed **(Sanborn et al., 2007)**. The authors contribute this effect to the activation energy that is needed for isomerization and which, apparently is highest for dyes attached to 5' ssDNA. Furthermore their results suggest, that Cy3 bound to 5' ssDNA interacts with the first two or three terminal bases

resulting in a relatively high barrier for isomerization **(Sanborn et al., 2007)**. Although the nucleic acid duplexes generated after hybridization are hybrids of DNA and rRNA rather than dsDNA, this effect might still appear. The extend of a possible bonding-dependent influence for hybrid nucleic acid duplexes probably is dye-specific and needs to be experimentally assessed before raising further speculations.

Another possibility that could explain the deviation between calculated and practical brightness, might be due to quenching effects through ribosomal proteins as reported by **Yilmaz & Noguera (2004)**. However, in contrast to this finding, Behrens and colleagues brought evidence, that high protein concentrations within cells might as well prevent quenching of probe fluorescence *in situ*, as probes quenched upon hybridization to a guanine-rich region of purified RNA in solution were not quenched anymore upon FISH **(Behrens et al., 2004)**.

Ultimately it could also be the case that fluorescence was quenched due to deoxyguanosines present at the target's binding site as reported from several studies **(Crockett & Wittwer, 2001; Zahavy & Fox, 1999)**. Though the first position of the 3'-dangling end targeted by the EUB-mix is a C, the second base is represented by a deoxyguanosine which could, due to the different chemical composition of the fluorophores, lead to differently pronounced, dye-specific quenching events.

One possible explanation for the large deviation between calculated and experimentally tested fluorescence intensities of ATTO 532 and ATTO 594 in particular (Table 6) could be due to the fact that these dyes emit in the green and dark yellow spectra, respectively. According to **Marras and co-workers (2002)**, dyes that emit in the green and yellow wavelengths are generally more affected by nucleotide quenching than fluorophores that emit in the blue or red spectra. This assumption is further emphasized by our results, as ATTO 490LS and Dy-681 show the least signal reduction by a factor of 1.3 and 1.5, respectively, which is in congruence with the respective detection window which is found within the red and dark red spectra. ATTO 633, which is detected in the light red wavelengths also follows the pattern mentioned above with a deviation factor of about 2.6. For ATTO 565, which is detected in the yellow spectra, this effect with a deviation factor of 3.1 is not as pronounced as one might have expected when focusing on the possibility of nucleotide quenching solely.

However, ATTO 565 together with ATTO 633 were the two brightest dyes among all tested fluorophores, exceeding the values of Cy3 by a factor of 1.55 and 1.45, respectively. The outstanding properties of ATTO 565 are also recognized in another study from 2011 where this dye yielded the highest overall fluorescence among 26 different organic dyes **(Dempsey et al., 2011)**. Additionally, these two dyes were successfully applied and compared to Cy3 in a previous study **(Ramesmayer, 2013).** According to the author, the fluorophores' brightness was comparable to, but not brighter than

the fluorescence emitted by the carbocyanine dye. It is noteworthy though, that this previous evaluation was based solely on subjective observations, rather than on exact measurements and therefore only represent an estimation.

Probably the effect of self-quenching as stated by **Fonin et al. (2014)** is also contemplable, albeit the respective proportions seek to be answered and are probably individual for each dye. The only dye for which self-quenching can be excluded very confidently is ATTO 490LS due to the stokes shift of 165 nm that separates the excitation and emission peaks too far from each other as to enable self-quenching (Fig 3). Furthermore, one has to consider that the theoretical fluorescence output per fluorophore provided by the companies are based on ultrapure ion water at pH optima, rather than on complex environmental samples and, due to the application of the Citifluor AF1 solution, at a pH of 9.

As Dy-681 and ATTO 490LS both possess a relatively low intrinsic quantum yield, and the latter one also has a low molar extinction coefficient, we expected them to be clearly below the total fluorescence intensity of Cy3. Additionally, it was not possible to excite Dy-681 at its adsorption maxima (691 nm), but rather 21 nm shifted towards the shorter wavelength, at 670nm. Although these two dyes clearly were the dimmest among all dyes investigated, they show the least deviation from theoretical fluorescence intensities. This (in comparison to the other dyes) relatively slight discrepancies between expected and measured fluorescence might be related to a reduced aggregation tendency in aqueous solutions as indicated by **Pauli et al., (2009)** and a reduced tendency for isomerization.

As it is apparently quite common in near- infrared fluorescence (NIRF) imaging, many researchers add bovine serum albumin (BSA) to the hybridization buffer in order to boost the overall fluorescence of the desired fluorophore **(Pauli et al., 2009; Philip et al., 1996; Sauda et al., 1986)**. According to the authors the fluorescence enhancement in the presence of BSA can be led back to BSA-binding induced rigidization of the dye molecules reducing cis-trans isomerizations **(Pauli et al., 2009)**. Furthermore the strong affinity of the dye to the BSA proteins shifts the onset of dimerization to higher concentrations resulting in a higher quantum yield **(Philip et al., 1996)**. It was shown, that by the addition of BSA to the PBS buffer, the quantum yield of Dy-681 could be raised from an initial value of 0.11 to 0.4, theoretically priming approximately a four times higher fluorescence. However, when doing so, it is recommended to readjust the excitation wavelength, since the absorption maxima will be red shifted in the presence of BSA **(Pauli et al., 2009)**. It would surely make sense to investigate this effect of BSA on the newly introduced fluorophores in a follow-up study, especially for those dyes that yielded relatively weak fluorescence intensities.

4.3 MULTICOLOUR FISH

The activated sludge sample used in this study to demonstrate the *in situ* applicability of the novel multicolor FISH approach was previously extensively investigated by 16S rRNA gene sequencing and FISH, with a specific focus on *Nitrospira*-microdiversity **(Gruber-Dorninger et al., 2015)**. Although the specific probes targeting closely related sublineages of *Nitrospira* belonging to the lineage I were already designed and optimized for FISH, the circumstance that this sludge sample clearly was dominated by *Nitrospira* affiliated with lineage II rather than with lineage I, complicated the attempt to visualize as many different *Nitrospira* subpopulations in one experiment (preferably within one field of view). Though this observation was for this purpose not confirmed by quantification, this clear trend could be observed by the naked eye, as lineage II *Nitrospira* were at least 10 times more abundant than lineage I *Nitrospira*. Furthermore, according to the author of the preceding *Nitrospira*-microdiversity study, the abundancies of lineage I and II *Nitrospira* were highly variable and depended on the time point of sampling **(Gruber-Dorninger et al., 2015).** Though this fact constituted a natural impediment that made successful screening for *Nitrospira* lineage I sub-clusters a bit tedious, it could be managed to capture six microbial taxa within one field of view (Fig 14-16). The two probes hybridized in a 3rd step at 25% FA (*Nitrospira* lineage I sub-clusters Ia and Ig) unfortunately, due to excessive washing-off of probes from previous hybridizations and massive depositions in the last hybridization, could not be captured in this very experiment. Instead images shown in Figure 16 are rather curtained during previous attempts where hybridization of the just mentioned were successful, but other probes partially failed to show signals.

The main aspect that complicated the visualization of all eight different taxa within one field of view clearly was the need for three consecutive hybridization steps. The reoccurring drying, hybridizing, washing and freezing events strongly decreased and sometimes even totally erased fluorescence. This was particularly pronounced for the Ntspa1131 probe from the first hybridization, but also for the Ntspa1431 and the AOB-mix. Signals obtained from the NOB-mix and the Ntspa1151 always exhibited clear (albeit weaker than after the 2nd hybridization) signals after the final hybridization. Since hindering effects (washing-off of probes & unspecific binding) can clearly be related to the multiple hybridization steps, it would surely increase the overall robustness of the protocol if one could decrease the latter to one single hybridization step. In case this is not feasible due to probe design, it could be beneficial to double label the probes applied in the first and second hybridization step and reduce hybridization times of subsequent hybridizations. Unfortunately, due to time limitations, it was not possible to further optimize the protocol and thus further raise the number of microbes for simultaneous detection. However, this new multicolour FISH approach clearly holds the potential for the simultaneous visualization of up to eight different microbial taxa per experiment/ field of view.

Despite all issues encountered, the advantages of this newly introduced multicolour FISH approach become obvious when comparing it to previous multicolour attempts. As in the CLASI-FISH approach **(Valm et al., 2011; Welch et al., 2016;)** two identical probes conjugated to two different fluorophores compete for the same target site, it is obvious that in the best case, this results in a 50% signal reduction for each dye and hence strongly decreases the overall sensitivity of the protocol. Furthermore it was shown, that binding affinities of probe-dye constructs are heavily dependent on the respective dye moieties **(Stoecker et al., 2010)**. Therefore, in practice, the binding ratio might be shifted towards the more competitive fluorophore, complicating unambiguous single cell detection. Even if two probes that target different regions of the same organisms are applied, the question remains whether it is technically feasible to design two different probes with same specificity and similar properties and behavior in regard to the hybridization condition. Even if probe design and an unambiguous assignment is feasible, this approach still is accompanied by very extensive and time-consuming standardization methods in order to obtain the respective label type of each binary combination, not to forget the necessity for the application of a linear unmixing algorithm. Finally, this approach exploits two fluorophores for identification of a single target which also makes this technique quite costly.

Also the protocols introduced by **Behnam et al. (2012)** and **Schimak and colleagues (2016)** are dependent on double, or even trinary labelling with different fluorophores. Not only are DOPE-probes almost twice as expensive as mono labelled probes, but also quenching effects that are individual for each dye combination might distort a reliable assignment. Thus, in order to guarantee a confident assignment, both approaches require a pre-evaluation on how each binary combination affects the fluorescence of the respective dyes. And although the approach introduced by **Amann and colleagues (1996)** does neither exploit multiple probes targeting one organism, nor binary dye combinations, this method is limited to the investigation of microbes that show high evolutionary conservation. Though it might work for the examination of closely related, nested population structures, this approach cannot be used for the analysis of phylogenetically widely separated microbial taxa which greatly diminishes the flexibility and possibilities of your experimental design.

In contrast to that, our newly introduced multicolour approach completely erases the possibility of wrong or ambiguous assignment, since neither binary dye combinations, nor multiple probes targeting a certain target are exploited. This further also eliminates the need for extensive pre-evaluations, standardizations or the development of a linear unmixing algorithm, and thus dramatically reduces the expenditure of work in the laboratory. Although we investigated microdiversity, and therefore used nested probes in our proof of principle samples, it is possible and likely even easier to detect 8 independent microbial populations with single, specific probes conjugated to the here introduced

alternative fluorophores. Ultimately, since probes are in general applicable as mono labelled oligonucleotides, this approach further displays and fairly economical alternative to the above mentioned previously established multicolor FISH approaches.

5. CONCLUSION

The here presented multicolor FISH approach is a fast, relatively easy-to-apply and straightforward method of simultaneous detection and spatial visualization of up to 8 microbial taxa, and will definitely take a shine to scientists dealing with the investigation of microscale biogeography **(Welch et al., 2016)** or the concept of microdiversity as introduced by **Moore et al. (1998)**. As microbes themselves serve as substrate for the attachment of other microbes, they hereby, through the excretion of various metabolites, also act as nutrient sources and hence might dramatically influence the physiology of surrounding organisms. Thus, this approach not only can help to visualize and resolve highly complex microbial interactions *in situ*, but also to gain a mechanistic understanding of the physiology of microbial key players, which strongly depends on organisms with which they commonly interact.

Especially within biofilms that are characterized by tight inter- and intraspecific microbial interactions and strong gradients of various gases and compounds such as oxygen or nitrogen species, this technique might further gain importance as it (e.g. through co-aggregation) might indicate hidden physiological potentials of important players one would overlook when examining a certain organism in isolation or under laboratory conditions. Also in regard to the investigation of the complex human gut microbiota or microbial consortia inhabiting the human's oral cavities (e.g. dental plaques), this approach, as it provides a framework for understanding the systems biology of the microbiome, further holds the potential to ameliorate and deepen our understanding about our microbial "roomies", which might ultimately have strong positive effects on the human health.

But also in regard to the 3D-FISH approach that uses embedding of the samples in polyacrylamide (PAA) gels in order to preserve the original architecture of e.g. activated sludge flocs **(Daims et al., 2006)**, the simultaneous investigation off more microbes might reveal previously unforeseen interactions and thus might be fruitful for raising assumptions that lead to new hypotheses.

To summarize, this newly introduced multicolour FISH approach clearly profits from its cost-, time- and labor-saving aspects and represents an easy-to-apply and straightforward technique with improved sensitivity. As the application is not limited to the investigation of microdiversity or biogeography, it will probably also be of great help for any studies dealing with the investigation of spatial structures and arrangements (with)in biological systems.

6. ZUSAMMENFASSUNG

Fluorescene *in situ* hybridization (FISH) mittels rRNA- gerichteten Oligonukleotidsonden ist ein sehr mächtiges und vielseitiges Tool für den Nachweis, die Visualisierung und der Quantifizierung von Mikroorganismen in umwelt- und medizinischen Proben. Da diese kultivierungsunabhängige Methode die Möglichkeit einer räumlichen Visualisierung der Anordnung von Mikroorganismen in ihrem Umfeld und zueinander ermöglicht, kann dadurch auf mögliche antagonistischen oder mutualistischen Lebensstile zurückgeschlossen werden. Daher stellt diese Technik eine wichtige Methode dar, die uns dabei hilft mehr Verständnis über die hochkomplexen, mikrobiellen Lebensgemeinschaften zu erfahren. Jedoch waren Wissenschaftler in der Vergangenheit durch intrinsische Limitationen von Mikroskopen (fixierte Anregungswellenlänge, Filter und Detektoren) auf die gleichzeitige Visualisierung von drei unterschiedlichen Taxa beschränkt. Wissenschaftler in der Vergangenheit haben versucht diese Limitation durch binäre Farbstoffkombinationen und der Verwendung von mehreren Sonden pro Zielorganismus zu umgehen, jedoch senken alle diese Methoden die Sensitivität des Protokolls beträchtlich, was schließlich zu falschen Zellzuordnungen führen kann. Daher stellen wir hier eine neue, robuste und leicht anwendbar FISH- Methode vor, bei der wir auf die neueste Technologie des Weißlichtlasers, mit seinen Möglichkeiten der stufenlosen Anregung- und Detektion zurückgreifen und diese mit alternativen Farbstoffen kombinieren. Als Bestätigung unseres Ansatzes haben wir die (Mikro-) Diversität einer nitrifizierenden Bakteriengesellschaft in einer Großkläranlage in Ingolstadt (Deutschland) visualisiert. Damit konnten acht verschiedene mikrobielle Gruppen erfasst werden, wobei es gelungen ist sechs Zielgruppen innerhalb eines Gesichtsfeldes zu visualisieren. Fluoreszenz Intensitätsmessungen haben weiteres ergeben, dass zwei alternative Farbstoffe die Leuchtkraft von Cy3 mit einem Faktor von 1,45 und 1,55 deutlich übersteigen. Daher bietet diese Arbeit nicht nur eine Reihe neuer, attraktiver und gut mit FISH kombinierbaren Farbstoffe an, sondern stellt es auch eine einfache, robuste und leicht anwendbare multicolour FISH Methode mit erhöhter Sensitivität dar, die sich besonders in der weiteren Erforschung von komplexen mikrobiellen Lebensgemeinschaften als dienlich erweisen wird.

7. ACKNOWLEDGMENT

My sincere thank goes to Assoc.-Prof. Dr. Holger Daims for giving me the opportunity to make my master thesis in his research group. Within the framework of my time in DOME, I could really gain a lot of experience in various scientific but also personal topics, and thanks to the offer of pretty free timing for my part, it also was possible to follow a side job besides my studies. Special thanks to Holger also for introducing me to the daime software, which was of great help for analysing my data.

Many thanks also to the head of our department, Prof. Dr. Dr. h. c. Michael Wagner for giving me the chance to use and be part of one of the most sophisticated microbial ecology research facilities in the world, hereby offering the unique possibility to look behind the scenes of high-end research.

Further I am grateful for all the patience, support, motivation and know-how from my supervisor Dr. Petra Pjevac. Without her, this study would probably never have come to an end. Thank you helping me to realize this big goal!

In this context, I would also show my great appreciation to Dr. Hanna Koch, my former supervisor who very nicely introduced me to all the skills, techniques and tricks required to work safely and efficiently in the lab. Also I very much appreciated her predilections for sarcasm, which were quite amusing throughout the sometimes quite exhausting lab work.

Many thanks also to Dr. Markus Schmid for sharing his expertise in regard to the CLSM with me and for a great personal introduction to the same. Furthermore, I would like to thank you (together with Petra Pjevac) for the preselection of all the alternative fluorophores that I evaluated throughout this study.

Also I want to thank Mag. rer. nat. Florian Wascher for always knowing what to do and helping me out when I was panicking at the CLSM. Many thanks also to Mag. rer. nat. Jasmin Schwarz who always was open to questions dealing with FISH or routine lab work. My appreciation also goes to Michael Lukumbuzya, MSc who performed cross-bleeding evaluations of alternative dyes on *E. coli*. Further I thank Raffaela Lesch for giving me a crash course into the GIMP software.

Finally, I would like to sincerely thank my parents for greatly supporting me financially and emotionally throughout my whole studies. Thank you from the bottom of my heart for always supporting and trusting in me, albeit I sometimes tend to strike unconventional paths. You always stood behind me, and I am convinced this will never change- whatever might come. Thank you for being such great parents- I couldn't wish for better ones- many thanks and love to both of you!

8. ABBREVIATIONS

3D - three-dimensional
AOB - ammonia oxidizing bacteria
AOBS - acousto-optical beam-splitter
AOTF - acousto-optical tunable filter
BSA - bovine serum albumin
CARD-FISH - catalyzed reported deposition FISH
CLASI-FISH - Combinatorial Labeling and Spectral Imaging FISH
CLSM - confocal laser scanning microscopy
DAPI - 4,6- diamidino- 2- phenylindole
ddH2O - double distilled water
DNA - deoxyribonucleic acid
DOPE-FISH - double labeling of oligonucleotide probes used for FISH
dsDNA - double stranded deoxyribonucleic acid
E.coli - *Escherichia coli*
FA - formamide
Fig. - Figure
FISH - fluorescence *in situ* hybridization
FLUOS - 5(6)- carboxyfluorescein- N- hydroxysuccinimide ester
IPTG - isopropyl- b- D- thiogalactopyranoside
IQR - interquartile range
LNA - locked- nucleic- acid
LP - laser power
MAR-FISH - microautoradiography FISH
MIL-FISH - multilabelled FISH
mRNA - messenger ribonucleic acid
NOB - nitrite oxidizing bacteria
P - pinhole
PBS - phosphate buffered saline
PFA - paraformaldehyde
PNA - peptide nucleic acid
RATS - rapid automated threshold selection
rDNA - ribosomal deoxyribonucleic acid
rRNA - ribosomal ribonucleic acid
SG - smartgain
ssDNA - single stranded DNA
UV - ultraviolet
WLL - white light laser
WWTP - wastewater treatment plant

9. REFERENCES

Adamczyk, J., Hesselsoe, M., Iversen, N., Horn, M., Lehner, A., Nielsen, P. H., … Wagner, M. (2003). The Isotope Array, a New Tool That Employs Substrate-Mediated Labeling of rRNA for Determination of Microbial Community Structure and Function. *Applied and Environmental Microbiology*, *69*(11), 6875–6887. http://doi.org/10.1128/AEM.69.11.6875-6887.2003

Amann, R. (1995). Fluorescently labelled , rRNA-targeted oligonucleotide probes in the study of microbial ecology. *Molecular Ecology*, *4*(January), 543–554. http://doi.org/10.1111/j.1365-294X.1995.tb00255.x

Amann, R. I., Binder, B. J., Olson, R. J., Chisholm, S. W., Devereux, R., & Stahl, D. A. (1990). Combination of 16S rRNA-targeted oligonucleotide probes with flow cytometry for analyzing mixed microbial populations. *Appl. Envir. Microbiol.*, *56*(6), 1919–1925. Retrieved from http://aem.asm.org/content/56/6/1919.short

Amann, R. I., Krumholz, L., & Stahl, D. A. (1990). Fluorescent-olignucleotide probing of whole cells for determinitive, phylogenetic, and environmental studies in microbiology. *Journal of Bacteriology*, *172*(2), 762–770.

Amann, R. I., Ludwig, W., Schleifer, K. H., Amann, R. I., & Ludwig, W. (1995). Phylogenetic identification and in situ detection of individual microbial cells without cultivation . Phylogenetic Identification and In Situ Detection of Individual Microbial Cells without Cultivation. *Microbiological Reviews*, *59*(1), 143–169. http://doi.org/10.1016/j.jip.2007.09.009

Amann, R. I., Snaidr, J., Wagner, M., Ludwig, W. G., & Schleifer, K. H. (1996). In situ visualization of high genetic diversity in a natural microbial community. *Journal of Bacteriology*, *178*(12), 3496–3500.

Amann, R., Snaidr, J., Wagner, M., & Ludwig, W. (1996). In Situ Visualization of High Genetic Diversity in a Natural Microbial Community, *178*(12), 3496–3500.

Ban, N., Nissen, P., Hansen, J., Capel, M., Moore, P. B., & Steitz, T. a. (1999). Placement of protein and RNA structures into a 5 A-resolution map of the 50S ribosomal subunit. *Nature*, *400*(6747), 841–847. http://doi.org/10.1038/23641

Behnam, F., Vilcinskas, A., Wagner, M., & Stoeckerb, K. (2012). A straightforward DOPE (double labeling of oligonucleotide probes)-FISH (fluorescence in situ hybridization) method for simultaneous multicolor detection of six microbial populations. *Applied and Environmental Microbiology*, *78*(15), 5138–5142. http://doi.org/10.1128/AEM.00977-12

Behrens, S., Fuchs, B. M., & Amann, R. (2004). The effect of nucleobase-specific fluorescence quenching on in situ hybridization with rRNA-targeted oligonucleotide probes. *Systematic and Applied Microbiology*, *27*(5), 565–72. http://doi.org/10.1078/0723202041748136

Behrens, S., Rühland, C., Inácio, J., Fonseca, Á., Fuchs, B. M., Amann, R., & Ru, C. (2003). In Situ Accessibility of Small-Subunit rRNA of Members of the Domains Bacteria , Archaea , and Eucarya to Cy3-Labeled Oligonucleotide Probes In Situ Accessibility of Small-Subunit rRNA of Members of the Domains Bacteria , Archaea , and Eucarya to Cy3-Labe, *69*(3), 1748–1758. http://doi.org/10.1128/AEM.69.3.1748

Binder, B. J., & Liu, Y. C. (1998). Growth Rate Regulation of rRNA Content of a MarineSynechococcus (Cyanobacterium) Strain. *Applied and Environmental Microbiology*, *64*(9), 3346–3351.

Borlinghaus, R. T., & Kuschel, L. R. (2012). The White Confocal – Spectral Gaps Closed, 809–817.

Brosius, J., Dull, T. J., Sleeter, D. D., & Noller, H. F. (1981). Gene organization and primary structure of a ribosomal RNA operon from Escherichia coli. *Journal of Molecular Biology*, *148*(2), 107–127. http://doi.org/10.1016/0022-2836(81)90508-8

Burggraf, S., Mayer, T., Amann, R., Schadhauser, S., Woese, C. R., & Stetter, K. O. (1994). Identifying members of the domain Archaea with rRNA-targeted oligonucleotide probes. *Applied and Environmental Microbiology*, *60*(9), 3112–3119.

Clemons, W. M., May, J. L., Wimberly, B. T., McCutcheon, J. P., Capel, M. S., & Ramakrishnan, V. (1999). Structure of a bacterial 30S ribosomal subunit at 5.5 A resolution. *Nature*, *400*(6747), 833–840. http://doi.org/10.1038/23631

Crockett, A. O., & Wittwer, C. T. (2001). Fluorescein-Labeled Oligonucleotides for Real-Time PCR: Using the Inherent Quenching of Deoxyguanosine Nucleotides. *Analytical Biochemistry*, *290*(1), 89–97. http://doi.org/10.1006/abio.2000.4957

Daims, H., Brühl, A., Amann, R., Schleifer, K. H., & Wagner, M. (1999). The domain-specific probe EUB338 is insufficient for the detection of all Bacteria: development and evaluation of a more comprehensive probe set. *Systematic and Applied Microbiology*, *22*(3), 434–44. http://doi.org/10.1016/S0723-2020(99)80053-8

Daims, H., Lücker, S., & Wagner, M. (2006). Daime, a Novel Image Analysis Program for Microbial Ecology and Biofilm Research. *Environmental Microbiology*, *8*(2), 200–213. http://doi.org/10.1111/j.1462-2920.2005.00880.x

Daims, H., Maixner, F., Lücker, S., Stoecker, K., Hace, K., & Wagner, M. (2006). Ecophysiology and niche differentiation of Nitrospira-like bacteria, the key nitrite oxidizers in wastewater treatment plants. *Water Science & Technology*, *54*(1), 21. http://doi.org/10.2166/wst.2006.367

Daims, H., Nielsen, J. L., Nielsen, P. H., Schleifer, K. H., & Wagner, M. (2001). In situ characterization of Nitrospira-like nitrite-oxidizing bacteria active in wastewater treatment plants. *Applied and Environmental Microbiology*, *67*(11), 5273–84. http://doi.org/10.1128/AEM.67.11.5273-5284.2001

Daims, H., Stoecker, K., & Wagner, M. (2005). Fluorescence in situ hybridization for the detection of prokaryotes. *Molecular Microbial Ecology*. Retrieved from http://books.google.com/books?hl=en&lr=&id=ciqAq2g5nPUC&oi=fnd&pg=PA192&dq=Fluorescence+In+Situ+Hybridization+For+The+Detection+Of+Prokaryotes&ots=GRBN18wPOl&sig=zSOSTyIpU2QhCFjCfAJefnkZOzE

Daims, H., & Wagner, M. (2011). *In Situ Techniques and Digital Image Analysis Methods for Quantifying Spatial Localization Patterns of Nitrifiers and Other Microorganisms in Biofilm and Flocs*. *Methods in Enzymology: Research on Nitrification and Related Processes Part B* (1st ed., Vol. 496). Elsevier Inc. http://doi.org/10.1016/B978-0-12-386489-5.00008-7

Delong, E. F., Taylor, L. T., Marsh, T. L., Preston, C. M., & Long, E. F. D. E. (1999). Visualization and Enumeration of Marine Planktonic Archaea and Bacteria by Using Polyribonucleotide Probes and Fluorescent In Situ Hybridization Visualization and Enumeration of Marine Planktonic Archaea and Bacteria by Using Polyribonucleotide Probes and, *65*(12), 5554–5563.

DeLong, E., Wickham, G., & Pace, N. (1989). Phylogenetic stains: ribosomal RNA-based probes for the identification of single cells. *Science*, *243*(4896), 1360–1363. http://doi.org/10.1126/science.2466341

Dempsey, G. T., Vaughan, J. C., Chen, K. H., Bates, M., & Zhuang, X. (2011). Evaluation of fluorophores for optimal performance in localization-based super-resolution imaging. *Nature Methods*, *8*(12), 1027–36. http://doi.org/10.1038/nmeth.1768

Dickinson, M. E., Bearman, G., Tille, S., Lansford, R., & Fraser, S. E. (2001). Multi-spectral imaging and linear unmixing add a whole new dimension to laser scanning fluorescence microscopy. *BioTechniques*, *31*(6), 1272, 1274–6, 1278. Retrieved from https://www.researchgate.net/publication/11588497_Multi-spectral_imaging_linear_unmixing_add_a_whole_new_dimension_to_laser_scanning_fluorescence_microscopy

Fahrmeir, L., Künstler, R., Pigeot, I., & Tutz, G. (2007). *Statistik: Der Weg zur Datenanalyse*. Retrieved from https://books.google.com/books?hl=de&lr=&id=fbIlBAAAQBAJ&pgis=1

Flardh, K., Cohen, P. S., & Kjelleberg, S. (1992). Ribosomes exist in large excess over the apparent demand for protein synthesis during carbon starvation in marine Vibrio sp. strain CCUG 15956. *J. Bacteriol.*, *174*(21), 6780–6788. Retrieved from http://jb.asm.org/content/174/21/6780.short

Fonin, A. V, Sulatskaya, A. I., Kuznetsova, I. M., & Turoverov, K. K. (2014). Fluorescence of dyes in solutions with high absorbance. Inner filter effect correction. *PloS One*, *9*(7), e103878. http://doi.org/10.1371/journal.pone.0103878

Fox, G. E., Pechman, K. R., & Woese, C. R. (1977). Comparative Cataloging of 16S Ribosomal Ribonucleic Acid: Molecular Approach to Procaryotic Systematics. *International Journal of Systematic Bacteriology*, *27*(1), 44–57. http://doi.org/10.1099/00207713-27-1-44

Fuchs, B. M., Glöckner, F. O., Wulf, J., & Glo, F. O. (2000). Unlabeled Helper Oligonucleotides Increase the In Situ Accessibility to 16S rRNA of Fluorescently Labeled Oligonucleotide Probes Unlabeled Helper Oligonucleotides Increase the In Situ Accessibility to 16S rRNA of Fluorescently Labeled Oligonucleotide Prob, *66*(8), 3603–3607. http://doi.org/10.1128/AEM.66.8.3603-3607.2000.Updated

Fuchs, B. M., Syutsubo, K., Ludwig, W., & Amann, R. (2001). In Situ Accessibility of Escherichia coli 23S rRNA to Fluorescently Labeled Oligonucleotide Probes In Situ Accessibility of Escherichia coli 23S rRNA to Fluorescently Labeled Oligonucleotide Probes, *67*(2), 961–968. http://doi.org/10.1128/AEM.67.2.961

Fuchs, B. M., Wallner, G., Beisker, W., Schwippl, I., Ludwig, W., & Amann, R. (1998). Flow Cytometric Analysis of the In Situ Accessibility of Escherichia coli 16S rRNA for Fluorescently Labeled Oligonucleotide Probes. *Appl. Envir. Microbiol.*, *64*(12), 4973–4982. Retrieved from http://aem.asm.org/content/64/12/4973.short

Fuhrman, J. A., & Campbell, L. (1998). Marine ecology: Microbial microdiversity, *393*(6684), 410–411. http://doi.org/10.1038/30839

Garcia-Martinez, J., & Rodriguez-Valera, F. (2000). Microdiversity of uncultured marine prokaryotes: the SAR11 cluster and the marine Archaea of Group I. *Molecular Ecology*, *9*(7), 935–948. http://doi.org/10.1046/j.1365-294x.2000.00953.x

Garini, Y., Young, I. T., & McNamara, G. (2006). Spectral imaging: principles and applications. *Cytometry. Part A : The Journal of the International Society for Analytical Cytology*, *69*(8), 735–47. http://doi.org/10.1002/cyto.a.20311

Giovannoni, S. J., DeLong, E. F., Olsen, G. J., & Pace, N. R. (1988). Phylogenetic group-specific oligonucleotide probes for identification of single microbial cells. *Journal of Bacteriology*, *170*(2), 720–726.

Glöckner, F. O., Amann, R., Alfreider, A., Pernthaler, J., Psenner, R., Trebesius, K., & Schleifer, K.-H. (1996). An In Situ Hybridization Protocol for Detection and Identification of Planktonic Bacteria. *Systematic and Applied Microbiology*, *19*(3), 403–406. http://doi.org/10.1016/S0723-2020(96)80069-5

Gruber-Dorninger, C., Pester, M., Kitzinger, K., Savio, D. F., Loy, A., Rattei, T., … Daims, H. (2015). Functionally relevant diversity of closely related Nitrospira in activated sludge. *The ISME Journal*, *9*(3), 643–55. http://doi.org/10.1038/ismej.2014.156

Harris, S. E., & Wallace, R. W. (1969). Acousto-Optic Tunable Filter. *J. Opt. Soc. Am.*, *59*(6), 744–747. http://doi.org/10.1364/josa.59.000744

Hoshino, T., Yilmaz, L. S., Noguera, D. R., Daims, H., & Wagner, M. (2008). Quantification of target molecules needed to detect microorganisms by fluorescence in situ hybridization (FISH) and catalyzed reporter deposition-FISH. *Applied and Environmental Microbiology*, *74*(16), 5068–5077. http://doi.org/10.1128/AEM.00208-08

Huang, W. E., Stoecker, K., Griffiths, R., Newbold, L., Daims, H., Whiteley, A. S., & Wagner, M. (2007). Raman-FISH: Combining sTable-isotope Raman spectroscopy and fluorescence in situ hybridization for the single cell analysis of identity and function. *Environmental Microbiology*, *9*(8), 1878–1889. http://doi.org/10.1111/j.1462-2920.2007.01352.x

Jaspers, E., & Overmann, J. (2004). Ecological significance of microdiversity: identical 16S rRNA gene sequences can be found in bacteria with highly divergent genomes and ecophysiologies. *Applied and Environmental Microbiology*, *70*(8), 4831–9. http://doi.org/10.1128/AEM.70.8.4831-4839.2004

Juretschko, S., Timmermann, G., Schmid, M., Schleifer, K., & Pommerening-ro, A. (1998). Combined Molecular and Conventional Analyses of Nitrifying Bacterium Diversity in Activated Sludge : Nitrosococcus mobilis and Nitrospira -Like Bacteria as Dominant Populations, *64*(8), 3042–3051.

Kashtan, N., Roggensack, S. E., Rodrigue, S., Thompson, J. W., Biller, S. J., Coe, A., … Chisholm, S. W. (2014). Single-cell genomics reveals hundreds of coexisting subpopulations in wild Prochlorococcus. *Science (New York, N.Y.)*, *344*(6182), 416–20. http://doi.org/10.1126/science.1248575

Kempf, V. a, Trebesius, K., & Autenrieth, I. B. (2000). Fluorescent In situ hybridization allows rapid identification of microorganisms in blood cultures. *Journal of Clinical Microbiology*, *38*(2), 830–8. Retrieved from http://www.pubmedcentral.nih.gov/articlerender.fcgi?artid=86216&tool=pmcentrez&rendertype=abstract

Kittler, J., Illingworth, J., & Föglein, J. (1985). Threshold selection based on a simple image statistic. *Computer Vision, Graphics, and Image Processing*, *30*(2), 125–147. http://doi.org/10.1016/0734-189X(85)90093-3

Krause, W. (Ed.). (2002). *Contrast Agents II* (Vol. 222). Berlin, Heidelberg: Springer Berlin Heidelberg. http://doi.org/10.1007/3-540-46009-8

Kubota, K., Ohashi, A., Imachi, H., & Harada, H. (2006). Improved in situ hybridization efficiency with locked-nucleic-acid-incorporated DNA probes. *Applied and Environmental Microbiology*, *72*(8), 5311–5317. http://doi.org/10.1128/AEM.03039-05

Kumar, Y., Westram, R., Behrens, S., Fuchs, B., Glöckner, F. O., Amann, R., … Ludwig, W. (2005). Graphical representation of ribosomal RNA probe accessibility data using ARB software package. *BMC Bioinformatics*, *6*, 61. http://doi.org/10.1186/1471-2105-6-61

Lee, N., Nielsen, P. H., Andreasen, K. H., Juretschko, S., Nielsen, J. L., Schleifer, K. H., & Wagner, M. (1999). Combination of fluorescent in situ hybridization and microautoradiography-a new tool for structure-function analyses in microbial ecology. *Applied and Environmental Microbiology*, *65*(3), 1289–97. Retrieved from http://www.ncbi.nlm.nih.gov/pubmed/10049895\nhttp://www.pubmedcentral.nih.gov/articlerender.fcgi?artid=PMC91176

Li, T., Wu, T. Di, Maz??as, L., Toffin, L., Guerquin-Kern, J. L., Leblon, G., & Bouchez, T. (2008). Simultaneous analysis of microbial identity and function using NanoSIMS. *Environmental Microbiology*, *10*(3), 580–588. http://doi.org/10.1111/j.1462-2920.2007.01478.x

Lübke, J. (1993). Photoconversion of diaminobenzidine with different fluorescent neuronal markers into a light and electron microscopic dense reaction product. *Microscopy Research and Technique*, *24*(1), 2–14. http://doi.org/10.1002/jemt.1070240103

Maixner, F., Noguera, D. R., Anneser, B., Stoecker, K., Wegl, G., Wagner, M., & Daims, H. (2006). Nitrite concentration influences the population structure of Nitrospira-like bacteria. *Environmental Microbiology*, *8*(8), 1487–95. http://doi.org/10.1111/j.1462-2920.2006.01033.x

Mark Welch, J. L., Rossetti, B. J., Rieken, C. W., Dewhirst, F. E., & Borisy, G. G. (2016). Biogeography of a human oral microbiome at the micron scale. *Proceedings of the National Academy of Sciences*, 201522149. http://doi.org/10.1073/pnas.1522149113

Marras, S. a E., Kramer, F. R., & Tyagi, S. (2002). Efficiencies of fluorescence resonance energy transfer and contact-mediated quenching in oligonucleotide probes. *Nucleic Acids Research*, *30*(21), e122. http://doi.org/10.1093/nar/gnf121

Mobarry, B., Wagner, M., Urbain, V., Rittmann, B., & Stahl, D. (1996). Phylogenetic probes for analyzing abundance and spatial organization of nitrifying bacteria [published erratum appears in Appl Environ Microbiol 1997 Feb;63(2):815]. *Appl. Envir. Microbiol.*, *62*(6), 2156–2162. Retrieved from http://aem.asm.org/content/62/6/2156.short

Moore, L. R., Rocap, G., & Chisholm, S. W. (1998). Physiology and molecular phylogeny of coexisting Prochlorococcus ecotypes. *Nature*, *393*(6684), 464–7. http://doi.org/10.1038/30965

Nazarenko, I., Pires, R., Lowe, B., & Rashtchian, A. (2002). Effect of primary and secondary structure of oligodeoxyribonucleotides on the fluorescent properties of conjugated dyes. *Nucleic Acids Research*, *30*(9), 2089–2095. http://doi.org/10.1093/nar/30.9.2089

Niemeyer, C. M., Bürger, W., & Peplies, J. (1998). Covalent DNA-Streptavidin Conjugates as Building Blocks for Novel Biometallic Nanostructures. *Angewandte Chemie International Edition*, *37*(16), 2265–2268. http://doi.org/10.1002/(SICI)1521-3773(19980904)37:16<2265::AID-ANIE2265>3.0.CO;2-F

Olsen, G. J., Lane, D. J., Giovannoni, S. J., & Pace, N. R. (1986). Microbial ecology and evolution: a ribosomal RNA approach. *Ann. Rev. Microbiol.*, *40*, 337–365.

Pauli, J., Brehm, R., Spieles, M., Kaiser, W. A., Hilger, I., & Resch-Genger, U. (2010). Novel fluorophores as building blocks for optical probes for in vivo near infrared fluorescence (NIRF) imaging. *Journal of Fluorescence*, *20*(3), 681–693. http://doi.org/10.1007/s10895-010-0603-7

Pauli, J., Vag, T., Haag, R., Spieles, M., Wenzel, M., Kaiser, W. A., … Hilger, I. (2009). An in vitro characterization study of new near infrared dyes for molecular imaging. *European Journal of Medicinal Chemistry*, *44*(9), 3496–503. http://doi.org/10.1016/j.ejmech.2009.01.019

Pawley, J. B. (2006). Points, pixels, and gray levels: digitizing image data. *Handbook of Biological Confocal Microscopy*, 59 – 79.

Pernthaler, A., & Amann, R. (2004). Simultaneous fluorescence in situ hybridization of mRNA and rRNA in environmental bacteria. *Applied and Environmental Microbiology*, *70*(9), 5426–33. http://doi.org/10.1128/AEM.70.9.5426-5433.2004

Pernthaler, A., Preston, C. M., Pernthaler, J., Delong, E. F., & Amann, R. (2002). Comparison of Fluorescently Labeled Oligonucleotide and Polynucleotide Probes for the Detection of Pelagic Marine Bacteria and Archaea Comparison of Fluorescently Labeled Oligonucleotide and Polynucleotide Probes for the Detection of Pelagic Marine Bacter. *Applied and Environmental Microbiology*, *68*(2), 661–667. http://doi.org/10.1128/AEM.68.2.661

Perry-O'Keefe, H., Rigby, S., Oliveira, K., Sørensen, D., Stender, H., Coull, J., & Hyldig-Nielsen, J. J. (2001). Identification of indicator microorganisms using a standardized PNA FISH method. *Journal of Microbiological Methods*, *47*(3), 281–292. http://doi.org/10.1016/S0167-7012(01)00303-7

Philip, R., Penzkofer, A., Bäumler, W., Szeimies, R. M., & Abels, C. (1996). Absorption and fluorescence spectroscopic investigation of indocyanine green. *Journal of Photochemistry and Photobiology A: Chemistry*, *96*(1-3), 137–148. http://doi.org/10.1016/1010-6030(95)04292-X

Ploem, J. (1999). Fluorescence microscopy. *Fluorescent and Luminescent Probes for Biological …*. Retrieved from https://books.google.at/books?hl=de&lr=&id=MWQVAMdoKmUC&oi=fnd&pg=PA3&dq=fluorescence+microscopy+ploem+1999&ots=gVfTzgbJlX&sig=ZT__kyqHRZImHGqQuDzBnG_A6eM

Ploem, J. S. (1987). Laser scanning fluorescence microscopy. *Applied Optics*, *26*(16), 3226–3231. http://doi.org/10.1364/AO.26.003226

R.R. Colwell, P.R. Brayton, D.J. Grimes, D.B. Roszak, S.A. Huq, and L. M. P. (1985). Viable but non-culturable vibriocholerae and related pathogens in the environment : implification for release of genetically engineerered microorganisms. *Nature*, *3*, 817–820.

Raghavachari, R. (2000). *Near-Infrared Applications in Biotechnology*. Retrieved from https://books.google.com/books?hl=de&lr=&id=R4xb4NPg8_kC&pgis=1

Randolph, J. B., & Waggoner, A. S. (1997). Stability, specificity and fluorescence brightness of multiply-labeled fluorescent DNA probes. *Nucleic Acids Research*, *25*(14), 2923–2929. http://doi.org/10.1093/nar/25.14.2923

Rietdorf, J., & Stelzer, E. H. K. (2006). Special optical elements. *Handbook of Biological Confocal Microscopy: Third Edition*, (c), 43–58. http://doi.org/10.1007/978-0-387-45524-2_3

Sanborn, M. E., Connolly, B. K., Gurunathan, K., & Levitus, M. (2007). Fluorescence properties and photophysics of the sulfoindocyanine Cy3 linked covalently to DNA. *The Journal of Physical Chemistry. B*, *111*(37), 11064–74. http://doi.org/10.1021/jp072912u

Sauda, K., Imasaka, T., & Ishibashi, N. (1986). Determination of protein in human serum by high-performance liquid chromatography with semiconductor laser fluorometric detection. *Analytical Chemistry*, *58*(13), 2649–2653. http://doi.org/10.1021/ac00126a016

Schaechter, M., MaalOe, O., & Kjeldgaard, N. O. (1958). Dependency on Medium and Temperature of Cell Size and Chemical Composition during Balanced Growth of Salmonella typhimurium. *Journal of General Microbiology*, *19*(3), 592–606. http://doi.org/10.1099/00221287-19-3-592

Schimak, M. P., Kleiner, M., Wetzel, S., Liebeke, M., Dubilier, N., & Fuchs, M. (2016). MiL-FISH : Multilabeled Oligonucleotides for Fluorescence In Situ Hybridization Improve Visualization of Bacterial Cells, *82*(1), 62–70. http://doi.org/10.1128/AEM.02776-15.Editor

Schmid, M., Schmitz-Esser, S., Jetten, M., & Wagner, M. (2001). 16S-23S rDNA intergenic spacer and 23S rDNA of anaerobic ammonium-oxidizing bacteria: Implications for phylogeny and in situ detection. *Environmental Microbiology*, *3*(7), 450–459. http://doi.org/10.1046/j.1462-2920.2001.00211.x

Schönhuber, W., Fuchs, B., Juretschko, S., & Amann, R. (1997). Improved sensitivity of whole-cell hybridization by the combination of horseradish peroxidase-labeled oligonucleotides and tyramide signal amplification. *Applied and Environmental Microbiology*, *63*(8), 3268–3273.

Schramm, A., Fuchs, B. M., Nielsen, J. L., Tonolla, M., & Stahl, D. a. (2002). Fluorescence in situ hybridization of 16S rRNA gene clones (Clone-FISH) for probe validation and screening of clone libraries. *Environmental Microbiology*, *4*(11), 713–720. http://doi.org/10.1046/j.1462-2920.2002.00364.x

Southwick, P. L., Ernst, L. A., Tauriello, E. W., Parker, S. R., Mujumdar, R. B., Mujumdar, S. R., … Waggoner, A. S. (1990). Cyanine dye labeling reagents--carboxymethylindocyanine succinimidyl esters. *Cytometry*, *11*(3), 418–30. http://doi.org/10.1002/cyto.990110313

Spring, S., Amann, R., Ludwig, W., Schleifer, K.-H., & Petersen, N. (1992). Phylogenetic Diversity and Identification of Nonculturable Magnetotactic Bacteria. *Systematic and Applied Microbiology*, *15*(1), 116–122. http://doi.org/10.1016/S0723-2020(11)80147-5

Staley, J. T., & Konopka, A. (1985). Measurement of in situ activities of nonphotosynthetic microorganisms in aquatic and terrestrial habitats. *Annual Review of Microbiology*, *39*, 321–346. http://doi.org/10.1146/annurev.micro.39.1.321

Stoecker, K., Dorninger, C., Daims, H., & Wagner, M. (2010). Double labeling of oligonucleotide probes for fluorescence in situ hybridization (DOPE-FISH) improves signal intensity and increases rRNA accessibility. *Applied and Environmental Microbiology*, *76*(3), 922–926. http://doi.org/10.1128/AEM.02456-09

Torimura, M., Kurata, S., Yamda, K., Yokomaku, T., Kamgata, Y., Kanagawa, T., & Kurane, R. (2001). Fluorescence-Quenching Phenomenonby Photon-Induced Electron Transfer between Fluorescent Dye and a Nucleotide Base. *Analytical Sciences*, *17*(January), 155–160. http://doi.org/10.2116/analsci.17.155

Valm, A. M., Welch, J. L. M., Rieken, C. W., Hasegawa, Y., Sogin, M. L., Oldenbourg, R., … Borisy, G. G. (2011). Systems-level analysis of microbial community organization through combinatorial labeling and spectral imaging. *Proceedings of the National Academy of Sciences of the United States of America*, *108*(10), 4152–4157. http://doi.org/10.1073/pnas.1101134108

Wachman, E. S., Niu, W., & Farkas, D. L. (1997a). AOTF Microscope. *Biophysical Journal*, *73*(September).

Wachman, E. S., Niu, W., & Farkas, D. L. (1997b). AOTF Microscope, *73*(September).

WAGNER, M., AßMUS, B., HARTMANN, A., HUTZLER, P., & AMANN, R. (1994). In situ analysis of microbial consortia in activated sludge using fluorescently labelled, rRNA-targeted oligonucleotide probes and confocal scanning laser microscopy. *Journal of Microscopy*, *176*(3), 181–187. http://doi.org/10.1111/j.1365-2818.1994.tb03513.x

Wagner, M., Horn, M., & Daims, H. (2003). Fluorescence in situ hybridisation for the identification and characterisation of prokaryotes. *Current Opinion in Microbiology*, *6*(3), 302–309. http://doi.org/10.1016/S1369-5274(03)00054-7

Wagner, M., Rath, G., Amann, R., Koops, H.-P., & Schleifer, K.-H. (1995). In situ Identification of Ammonia-oxidizing Bacteria. *Systematic and Applied Microbiology*, *18*(2), 251–264. http://doi.org/10.1016/S0723-2020(11)80396-6

Wallner, G., Amann, R., & Beisker, W. (1993). Optimizing fluorescent in situ hybridization with rRNA-targeted oligonucleotide probes for flow cytometric identification of microorganisms. *Cytometry*, *14*(2), 136–43. http://doi.org/10.1002/cyto.990140205

Waters, J. C. (2009). Accuracy and precision in quantitative fluorescence microscopy. *The Journal of Cell Biology*, *185*(7), 1135–48. http://doi.org/10.1083/jcb.200903097

Wessendorf, M. W., & Brelje, T. C. (1992). Which fluorophore is brightest? A comparison of the staining obtained using fluorescein, tetramethylrhodamine, lissamine rhodamine, texas red, and cyanine 3.18. *Histochemistry*, *98*(2), 81–85. http://doi.org/10.1007/BF00716998

Woebken, D., Lam, P., Kuypers, M. M. M., Naqvi, S. W. A., Kartal, B., Strous, M., … Amann, R. (2008). A microdiversity study of anammox bacteria reveals a novel Candidatus Scalindua phylotype in marine oxygen minimum zones. *Environmental Microbiology*, *10*(11), 3106–19. http://doi.org/10.1111/j.1462-2920.2008.01640.x

Woese, C. R. (1987). Bacterial Evolution. *Microbiology*, *51*(2), 221–271. http://doi.org/10.1139/m88-093

Woese, C. R., & Fox, G. E. (1977). Phylogenetic structure of the prokaryotic domain: the primary kingdoms. *Proceedings of the National Academy of Sciences of the United States of America*, *74*(11), 5088–5090. http://doi.org/10.1073/pnas.74.11.5088

Worden, A. Z., Chisholm, S. W., & Binder, B. J. (2000). In situ hybridization of Prochlorococcus and Synechoccus (marine cyanobacteria) spp. with rRNA-targed peptide nucleic acid probes. *Applied and Enviromental Microbiology*, *66*(1), 284–289.

Yarmoluk, S. M., Lukashov, S. S., Ogul'Chansky, T. Y., Losytskyy, M. Y., & Kornyushyna, O. S. (2001). Interaction of cyanine dyes with nucleic acids. XXI. Arguments for half-intercalation model of interaction. *Biopolymers - Biospectroscopy Section*, *62*(4), 219–227. http://doi.org/10.1002/bip.1016

Yilmaz, L. S., Bergsven, L. I., & Noguera, D. R. (2008). Systematic evaluation of single mismatch stability predictors for fluorescence in situ hybridization. *Environmental Microbiology*, *10*(10), 2872–85. http://doi.org/10.1111/j.1462-2920.2008.01719.x

Yilmaz, L. S., & Noguera, D. R. (2004). Mechanistic Approach to the Problem of Hybridization Efficiency in Fluorescent In Situ Hybridization. *Society*, *70*(12), 7126–7139. http://doi.org/10.1128/AEM.70.12.7126

Yilmaz, L. S., & Noguera, D. R. (2007). Development of thermodynamic models for simulating probe dissociation profiles in fluorescence in situ hybridization. *Biotechnology and Bioengineering*, *96*(2), 349–63. http://doi.org/10.1002/bit.21114

Yilmaz, L. S., Ökten, H. E., & Noguera, D. R. (2006). Making All Parts of the 16S rRNA of Escherichia coli Accessible In Situ to Single DNA Oligonucleotides Making All Parts of the 16S rRNA of Escherichia coli Accessible In Situ to Single DNA Oligonucleotides †. *Applied and Environmental Microbiology*, *72*(1), 733–44. http://doi.org/10.1128/AEM.72.1.733

Yilmaz, L. S., Parnerkar, S., & Noguera, D. R. (2011). MathFISH, a web tool that uses thermodynamics-based mathematical models for in silico evaluation of oligonucleotide probes for fluorescence in situ hybridization. *Applied and Environmental Microbiology*, *77*(3), 1118–1122. http://doi.org/10.1128/AEM.01733-10

Zahavy, E., & Fox, M. A. (1999). Photophysical Quenching Mediated by Guanine Groups in Pyrenyl-N-alkylbutanoamide End-Labeled Oligonucleotides. *J. Phys. Chem. B*, *103*(43), 9321–9327. http://doi.org/10.1021/jp9913822

Zarda, B., Amann, R., Wallner, G., & Schleifer, K. H. (1991). Identification of single bacterial cells using digoxigenin-labelled, rRNA-targeted oligonucleotides. *Journal of General Microbiology*, *137*(12), 2823–2830. http://doi.org/10.1099/00221287-137-12-2823

10. SUPPLEMENTARY INFORMATION

10. 1. MATERIALS

Table 7: Consumables and equipment used in this study.

Consumable	Manufacturer
Microscope slides (76 x 20 mm)	Paul Marienfeld GmbH & Co.KG
Cover glasses (50 x 24 mm ±170 µm)	Carl Roth GmbH
Waterbath (GFL L1004)	GFL®
Hybridization oven	Memmert
50 ml screw cap tubes	Greiner
Eppendofr Tubes, various sizes	Eppendorf
Glass bottles, screw- cap, various sizes	Schott
Tips, various sizes	Biozym Scientific GmbH
Eppendorf Research Pipettes, various sizes	Eppendorf
MQ Biocel (water purification system)	Merck Millipore
BL3100 and BL6100 (balance)	Sartorius
Centrifuge 5804R,, Eppendorf	Eppendorf
MiniSpin plus (microcentrifuge)	Eppendorf
DMI6000, TCS SP8 X	Leica
ProfiLine pH 3110 (pH- meter)	WTW
LE agarose	Biozym Scientific GmbH
Probes	Biomers
Vortex Genie 2	Scientific Industries
Citifluor AF1 solution	Agar Scientific
Ethanol denatured	AustroAlco

10.2. CHEMICALS AND SOLUTIONS FOR FISH

10 x PBS Stock:	NaCl: 80 g KCl: 2 g $Na_2HPO_4H_2O$: 18 g KH_2PO_4 : 2,4 g H_2O HCl (1M) adjust pH to 7,2- 7,4 dilute 10 x Stock solution 1:10 with dd_H20
5 M NaCl:	292,2 g/l H_2O fill up to 1 l
10 % SDS:	5 g SDS H_2O fill up to 50 ml
PFA:	21,6 ml formalin (37%) H_2O: 178,4 ml
0,5 M EDTA	$Na_2EDTA*2H_2O$: 46,5 g Adjust pH to 8 (NaOH)
1 M Tris/HCl	121,1 g/l Adjust pH to 8 (HCl)